T.C.
İSTANBUL UNIVERSITY
INSTITUTE OF GRADUATE STUDIES IN
SCIENCE AND ENGINEERING

M.Sc. THESIS

VIBRATIONAL SPECTROSCOPIC STUDY ON WATER COMPLEXES OF ETHIONAMIDE MOLECULE

Umaima Saleh Mahfouth ZERTİ

Department of Physics

Physics Programme

SUPERVISOR
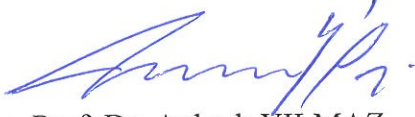**Prof. Dr. BAYRAM DEMİR**

June, 2018

İSTANBUL

This study was accepted on 8/6/2018 as a M. Sc. thesis in Department of Physics, Physics Programme by the following Committee.

Examining Committee Members

Prof. Dr. Bayram DEMİR(Supervisor)
İstanbul University
Faculty of Science

Assoc. Prof. Dr. Ayberk YILMAZ
İstanbul University
Faculty of Science

Assoc. Prof. Dr. Olcay BÖLÜKBAŞI
YALÇINKAYA
İstanbul University
Faculty of Science

Assist. Prof. Dr. Fatma AYDOĞMUŞ ŞEN
İstanbul University
Faculty of Science

Assist. Prof. Dr. Serpil ÇIKIT
Haliç University
Faculty of Art and Sciences

As required by the 9/2 and 22/2 articles of the Graduate Education Regulation which was published in the Official Gazette on 20.04.2016, this graduate thesis is reported as in accordance with criteria determined by the Institute of Graduate Sttudies in Science and Engineering by using the plagiarism software to which İstanbul University is a subscriber.

FOREWORD

I would like to thank my supervisor Prof. Dr. Bayram DEMİR, I would also like to thank express my gratitude and appreciation to Assoc. Prof. Dr. Ayberk YILMAZ for all the help and guidance he provided throughout my education. I would like to thank my family especially my husband for their. Encouragement, patience and assistance over the years. I forever indebted to my parents who have always kept me in their prayers.

June 2018   Umaima Saleh Mahfouth ZERTİ

TABLE OF CONTENTS

LIST OF FIGURES

LIST OF TABLES

LIST OF SYMBOLS AND ABBREVIATIONS

Symbol	Explanation
ϖ	: Oscillation Frequency
χ_e	: Anharmonicity Constant
k	: Spring Constant
A	: Bond Angle
R	: Bond Distance
o	: Angles
O_2	: Dioxygen
NO	: Nitric Oxide
v	: Frequency
C	: Speed Of Light
E	: Electric Field
H	: Magnetic Field
ν	: Stretching
δ	: In Plane Bending
γ	: Out Of Plane Bending
τ	: Torsion

Abbreviation	Explanation
ATR	: Attenuated Total Reflectance
BO	: Born Oppenheimer
ESR	: Electron Spin Resonance
FT	: Fourier Transform
FTIR	: Fourier Transform Infrared Spectroscopy
HF	: Hartree-Fock
IR	: Infrared
NMR	: Nuclear Magnetic Resonance
PED	: Potential Energy Distributions
QCD	: Quantum Chromo Dynamics

ÖZET

YÜKSEK LİSANS TEZİ

ETİONAMİD MOLEKÜLÜNÜN SU KOMPLEKSLERİ ÜZERİNE TİTREŞİM SPEKTROSKOPİSİ ÇALIŞMASI

Umaima Saleh Mahfouth ZERTİ

İstanbul Üniversitesi

Fen Bilimleri Enstitüsü

Fizik Anabilim Dalı

Danışman : Prof. Dr. Bayram DEMİR

Bu tezde, serbest etionamid (ETH) molekülü ve olası etionamid-su komplekslerinin optimize edilmiş geometri parametreleri DFT/B3LYP ile 6-31G (d, p) baz seti kullanılarak belirlenmiştir. Geometri optimizasyon hesaplamasından sonra, en kararlı ETH molekülünün ve su komplekslerinin harmonik titreşimsel dalgasayıları ve IR siddetleri hesaplanmıştır. Titreşim modlarının atanması potansiyel enerji dağılımına (PED) dayalı olarak gerçekleştirilmiştir. etionamid (ETH) molekülü ve olası etionamid-su komplekslerinin FT-IR(Fourier Dönüşümli Kırmızı-Altı) spektrumları ATR(Zayıflatılmış Toplam Yansıma) unitesi ile katı fazda 4000-400 cm^{-1} aralığında kayıt edilmiştir. Deneysel ve teorik olarak elde edilen spektrumlar karşılaştırarak, dalga boylarındaki ve şiddetlerdeki değişmeler incelendi.

Haziran 2018, 67 sayfa.

Anahtar kelimeler: Fourier Transform Infrared, Ethionamide, Attenuated Total Reflectance

SUMMARY

M.Sc. THESIS

VIBRATIONAL SPECTROSCOPIC STUDY ON WATER COMPLEXES OF ETHIONAMIDE MOLECULE

Umaima Saleh Mahfouth ZERTİ

İstanbul University

Institute of Graduate Studies in Science and Engineering

Department of Physics

Supervisor : Assoc. Prof. Dr. Bayram DEMİR

In this thesis, optimized geometry parameters of free ethionamide (ETH) molecule and its possible ethionamide-water complexes were determined by using DFT/ B3LYP with 6-31G(d,p) basis set. After geometry optimization calculation, the harmonic vibrational wavenumbers and IR intensities of the most stable ETH molecule and its water complexes were calculated. The assignment of the vibrational modes was performed based on the potential energy distribution (PED). FTIR (Fourier Transform Infrared) spectra of the ETH and ETH-water complex were recorded with an ATR (Attenuated Total Reflectance) unit in the regions 4000-400 cm^{-1} in the solid phase. By comparing the experimental and theoretical obtained spectra, the variations in wavenumbers and intensity were examined.

June 2018, 67 pages.

Keywords: Fourier Transform Infrared, Ethionamide, Attenuated Total Reflectance

1. INTRODUCTION

Today, tuberculosis remains an important public health problem all over the world (Zaman, 2010; Hershfield, 1991). It is estimated that one third of the world's population is currently infected with tuberculosis. One tenth of the individuals living in the population have risk of tuberculosis at any period of their life (Khasnobis, Escuyer, & Chatterjee, 2002; Dye et al., 1999). Long term use of many drugs in treatment of tuberculosis leads to serious problems in patients who are resistant to drugs used. It is therefore necessary to carry out studies aimed at the development of new tuberculosis drugs, which are effective in short term and easy to use (Hamilton, 1999; Banerjee et al., 1994).

Etionamide is a second line drug, which is used in conjunction with other drugs when primary drugs are not effective. Although the mechanism of its real effect is unknown, it is assumed that it is active by inhibiting mycotic synthesis in the mycobacterial cell wall as seen in isoniazid (Quemard, 1991; Schroeder, 2002). Studies in which the FTIR spectrum of the ETH molecule is studied and the DFT calculations are performed can be seen in the literature (Muthu & Ramachandran, 2002; Wysokiński et al., 2006).

Spectroscopy examines the interaction of light with the matter. Molecules make vibration, rotation, and reciprocating motion. Examination of intramolecular vibrational and rotational movements gives important information about the structure of molecules. The structure and the structural changes in any compound can be examined by the Infrared Spectroscopy method. The region 1200-600 cm^{-1} in Infrared Spectrum is called the fingerprint region and the region between 3600-1200 cm^{-1} is called the functional group which gives structural changes.

In theoretical part of this thesis, stable geometry and vibrational frequencies of Ethionamide (ETH) molecule and its H$_2$O complexes were calculated by Gaussian 09 program (Gaussian 09, Revision A.02, Gaussian Inc., Wallingford CT, 2009) with Density Functional Theory (DFT) method with 6-31G (d, p) basis set. In the experimental part of this study, FT-Mid IR spectra of the ETH ad ETH-water complex were recorded in the regions 4000-400 cm^{-1} in the solid phase. The comparison beteen calculated and experimental vibrational spectra and assignments of fundamental vibrational modes were characterized by Potential Energy Distribution (PED)

(Martin, J.M.L. and Alsenoy, C.V., GAR2PED, 1995). Molecular structures were visualized by Jmol program (Jmol, version 13.0, 2018).

2. MATERIALS AND METHODS

2.1. VIBRATIONAL SPECTROSCOPY

The term vibrational spectroscopy is defined as the combination of two different analytical techniques, namely Infrared(IR) spectroscopy and Raman spectroscopy (Sathyanarayana, 2015). These two techniques are used to analyze the molecular composition, their structure, and the how they interaction with a sample moreover, these tools are nondestructive and non-invasive. Further, IR spectroscopy and Raman spectroscopy are used to measure the vibrational energy levels that are related to chemical bonds of a sample. The spectrum of a sample is exclusive e.g., a fingerprint therefore, vibrational spectroscopy helps to assess the identity, character, elucidation structure, monitoring of reaction and quality control and assurance (Colthup, 2012).

As it has been as described in the first paragraph the complementary information about molecular structure is obtained through Infrared and Raman spectroscopy more specifically, any given example is irradiated by "polychromatic" light plus consequently absorbs the light of a photon while the frequency of the energy of that particular absorption matches with required vitality aimed at a specific "bond to vibrate" with that particular example is being explained by Infrared spectroscopy (Long & Long, 1977). On the other hand, Raman spectroscopy the particular example irradiated by "monochromatic" light plus led to scatter elastically and in-elastically the photons of light. Moreover, the consequent elastic scatter light contains equal level of dynamism that the incident light laser contains therefore, it is known as Rayleigh scatter. However, the in-elastic scattered light is called Raman Scatter that vanishes the strokes or achieve opposing strokes energy to interact and produce photons containing material that is describe as the structure of a molecule in the example.

Furthermore in Raman spectroscopy, the instruments that are designed in modern Raman spectroscopy help to filter the light (Rayleigh) for one photon from a sample of one million photons is referred to Raman scattered (Colthup, 2012). To be Raman active, one more requirement is the vibration and there must be a change in "polarisability" when molecule vibrate for example, a result in shape changes, electron cloud's size and orientation that surrounds the molecules.

To make the subject clear, Figure 2.1 is presented where Infrared and Raman data shown in a spectrum below:
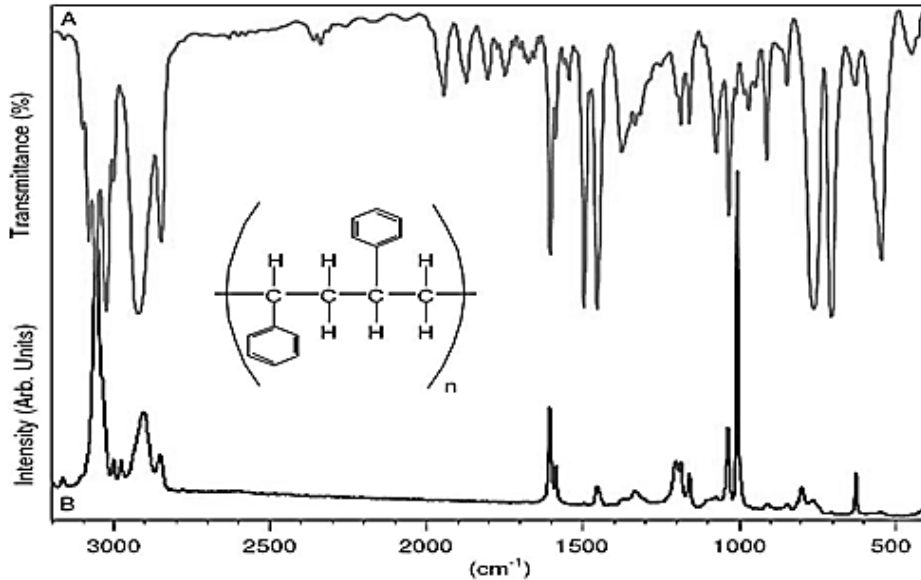
Figure 2.1: Infrared (A) and Raman (B) spectra of polystyrene.

In the Figure 2.1, it can be seen clearly that a sample is absorbing or transmitting a certain amount of light in contradiction of a certain level of energy. Consequently, the Raman shift is stated as an intensity plot that contains the dispersed light against the changes in energy that can also be stated as cm^{-1}.

2.2. FOURIER TRANSFORMED INFRARED SPECTROSCOPY (FTIR)

The technique of FTIR helps to get the ultraviolet range of absorption or emission of a substance that can be a solid, liquid or gas (Faix, 1992). Moreover, over a wide spectral range, FTIR spectrometer is used to collect extraordinary resolution data, simultaneously. On the other hand, a dispersive spectrometer lacks to measure the high spectral resolution data and only measures the wavelengths at a point with very thin array thus, it deliberates an advantage over a dispersive spectrometer.

The general term Fourier spectroscopy refers to analyzing whichever fluctuating signals into their essential components of frequency. The application of Fourier transformed is wide and range from infrared spectroscopy that is also known as FTIR, nuclear magnetic resonance (NMR), and electron spin resonance (ESR) spectroscopy. Moreover, Fourier transformation of

an optical interferogram helps to obtain FTIR spectroscopy that includes absorption, reflection, emission, or photoacoustic spectrum. A simultaneous analysis of several components at the same time in one operation makes this method a powerful tool. The application of concepts of Fourier to spectroscopy generates spectrometer by powerful technology which initiates the whole spectrum that otherwise in a traditional spectrometer i.e. prism and grating has to scan only a single line in a given spectrum. Therefore, the effectiveness of Fourier spectrometer is obvious in its speed to utilize the interferometers through a factor identical to several elements that are resolvable in a given spectrum. Moreover, the use of Fourier based methods have a wide range of application over the spectrum.

The application of FT spectroscopy ranges from the long variety of frequency that varies across ultraviolet, visible, infrared near, mid-infrared, and even include the far-infrared regions. The selection of the regions depends on diverse beam splitters and detectors for respective ranges of the regions. It is pertinent to mention here that there is no other technique available that could study the variety of the frequency across a wide range of regions. However, there are several spectroscopy techniques that are used to study various samples, though the popularity and usage of FTIR spectroscopy is the highest. Most important reasons behind the extensive usage of FTIR spectroscopy are its ability to generate speed, accuracy and the sensitive results that would not be possible earlier.

FTIR spectroscopy makes it possible to study and analyze the micro-samples in particular cases at the level of monogram and therefore it is a priceless tool to solve the problems in several studies. It is important to note that the application of the FTIR spectroscopy is different from the traditional dispersive techniques of spectroscopy based on the principles differences therefore, the perfect use of FTIR depends on the careful study of these principles.

The difference between the traditional wave spectrometer and the FTIR spectroscopy is based on different principles as in traditional wave spectroscopy the electromagnetic radiation is being exposed to the particular sample and the transmission of the radiation is measured on the basis of the intensity and respectively monitored. Resultantly, there is a variation in the incident radiation energy across the anticipated range and the function of incident radiation frequency plot the response. The resonant occurrences that are considered characteristics of the sample are used to identify the sample and are determined through the absorbed radiation that results in several peaks in the respective spectrum. However, FTIR spectroscopy instead of electromagnetic radiation exposure to the particular sample and the transmission of the radiation

of the intensity is exposed to single pulse of radiation that consists of several frequencies in the given range. Thus, in FTIR, the subsequent signals contain the rapid decay compound of all possible frequencies. Moreover, the application of the Fourier transformation spectrometer on the signal will generate the sample resonance and the respective frequencies dominate the signal. This process then helps to calculate the response on the frequencies. Therefore, the production of the spectrum could be same in the FTIR and the traditional spectrometer but the only difference is the time.

The use of interferometers is different from every FTIR spectrometer, for instance, the Michelson interferometer, lamellar grating, and Fabry-Perot interferometer. The Michelson interferometer and lamellar grating interferometer are the beam interferometers and have a high power to resolve compared to the Fabry-Perot interferometer that basically utilize the low resolving power. It is important to note that all the interferometers have their own advantages and disadvantages particularly the beam interferometers.

The basic difference between the two beam interferometers is the in Michelson interferometer the wave amplitude occurs while on the other hand, the lamellar grating spectrometer occur wave-front divisions. Moreover, the Michelson interferometer is more famous compared to the lamellar grating because it is easy to construct and operate. Additionally, the available commercial FTIR spectrometers use Michelson interferometer because they are more advantageous over the other available interferometers on the basis of high energy output, multiplex, and extraordinary accuracy in the measurement of the frequencies.

The FTIR spectroscopy has a main advantage that differentiates it from the others is the interferometer that produces first relative to a spectrum and there is little information to be obtained from the given interferometer deprived of further dispensation. A computer is necessary to convert the interferogram to a spectrum using Fourier analysis. The rapid technological developments help a lot for the growth of FTIR spectroscopy and it has ruled out the presence of any type of technical difficulties to transform the numbers of a big data points. For example, 10^6 sample transformations will only take few seconds on computer to calculate.

It is important to note despite the technological advantages in performing the Fourier spectroscopy, there exists a major difficult that is the accurate understanding of the interferogram. However, the use and application of the FTIR spectroscopy is widely used technique to measure the infrared absorption (IR) and spectrum emission. Moreover, one of the

major advantages of the use of FTIR method over the dispersive spectroscopy is visible characteristics of all the absorptions/emissions in the spectral region of the IR, thus, the calculation of is possible in both quantitative and qualitative ways. Though, FTIR is still considered a new approach despite its expansion over the past two decades.

Besides the advantages and dominance of FTIR over the traditional spectroscopy methods, it is important to discuss the how FTIR generate the spectrum, the main principle and the theory. The two basic parts of the FTIR spectrometer consists of the utilization of the interferometer and a computer. The use of minicomputer to generate the digital infrared spectrum information is the main advantage, however, the actual advantage of FTIR is the attainment of the interferometer through spectrometer compared to the traditional spectrometer through prism or grating. Therefore, to better represent the FTIR spectroscopy, a Figure 2.2 highlight the three optical inputs that consists HeNe laser, white light, and the source of infrared that connect to the interferometer.

The use of computer is very significant in terms of controlling the optical components, collection and storing of data, making calculations and analysis on the data, and displaying the spectra. Moreover, the direct use and interference of the computer to the spectrometer helps to arithmetically manipulate the spectra, for instance, the subtraction of composite spectra can support to eliminate the interface absorption.

FTIR has analytical applications that can help to recognize both organic and inorganic materials and the measurement of infrared radiation absorption using sample material against wavelength, and structures and components of a molecular it also stimulates the high tremor state of particles while absorbing infrared radiation (IR) when a material irradiated with IR. It is particular to mention here that a specific molecule refers to the different levels of energy among indifferent and agitated states of vibration and absorbs wavelength of light (Jaggi & Vij, 2006). The sample absorbs the wavelength which is molecular structure characteristics.

The wavelength from a broadband infrared source is modulated by an interferometer that a FTIR spectrometer uses. The intensity of transmission and reflection of light is measured by a detector and it is a function of wavelength. The signal that is being captured by a detector which is called interferogram, and it can be analyzed using fourier transformation obtaining a single beam infrared spectrum with a computer (Smith, 2011).

During the process of the infrared spectrum, the second stage of the technique is to interpret. The interpretation of spectrum is simple because the appeared bands could be assigned to the respective molecule that resultantly produces the group frequencies. This allows us to discuss the characteristics of group frequency that are observed in different regions. This section briefly discusses the mid-infrared region, near-infrared region and far-infrared region.
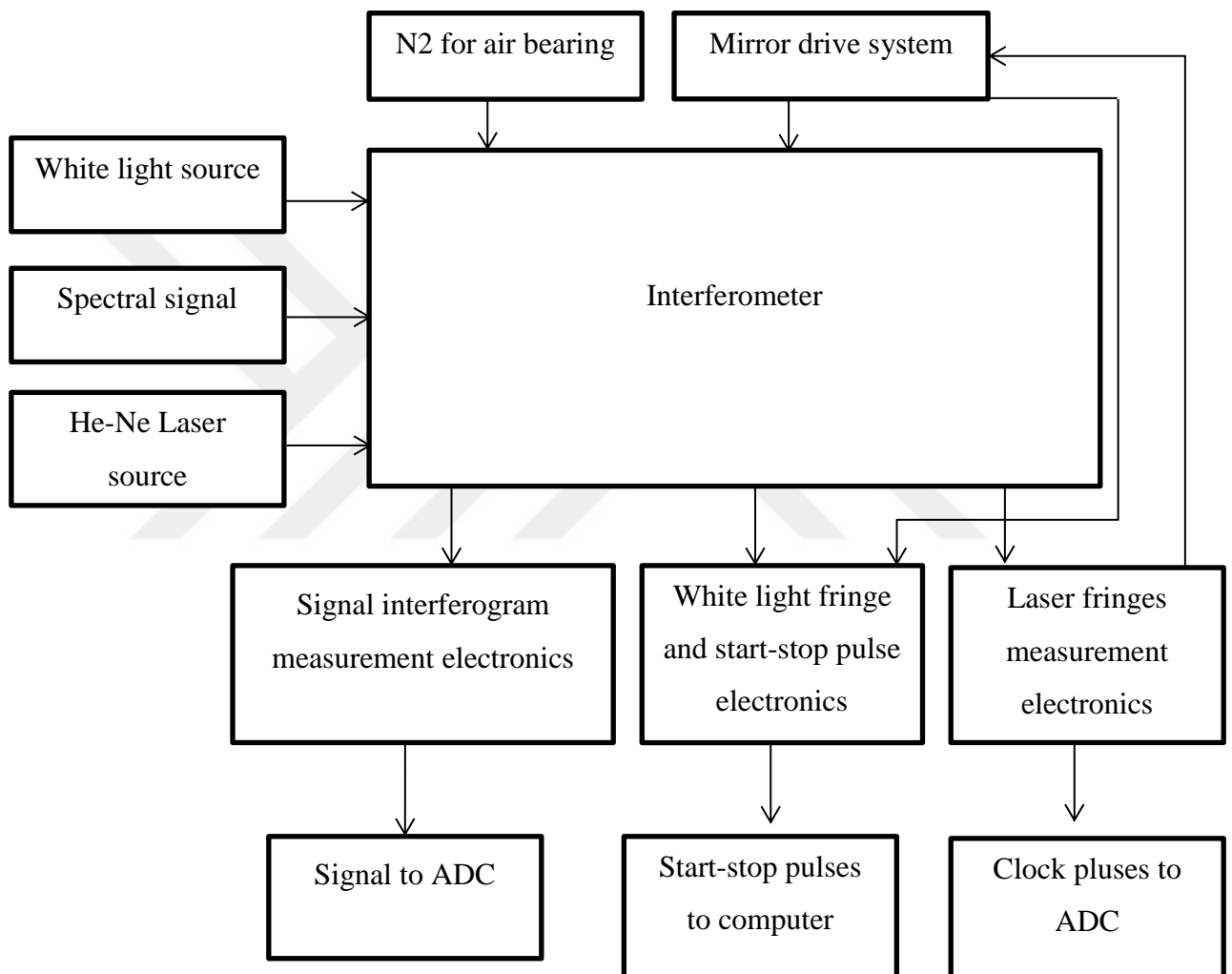
Figure 2.2: FTIR spectrometer block diagram.

2.2.1. Mid-Infrared Region

The approximate division of the mid-infrared region spans over $(4000 – 400\,cm^{-1})$ and it divides into four regions moreover, the group frequency nature depends in the location of the region. The generalization of the region as follows:

The X-H stretching region $(4000 – 2500\,cm^{-1})$

The triple-bond region $(2500 - 2000\,cm^{-1})$

The double-bond region $(2000 - 1500\,cm^{-1})$

The fingerprint region $(1500 - 600\,cm^{-1})$

2.2.2. Near-Infrared Region

The near-infrared region contains the observations of absorption $(13000 – 40000\,cm^{-1})$ that is implies and combines the important stretching bands that happen in the $(3000 – 100\,cm^{-1})$.
The occurring of the band happens because of C – H OR N – H OR O – H stretching . The bands involved in the near-infrared region that are close to infrared are usually less intensive and it is a decreasing trend of factor of 10 with each overtone to the next.

It is important to note that the existence of the bands in the near-infrared region are overlapping and make bands less useful compared to the mid-infrared region in the context of qualitative analysis. However, the difference between the near and mid infrared positions exists for different functional groups. Moreover, it is possible to exploit these differences for the qualitative analyze the bands.

2.2.3. Far-Infrared Region

The region of far-infrared ranges from   400 and 100 cm^{-1} and it is very limited compared to mid-infrared correlations of structure and spectra, however, there is no explanation provided on the molecular vibration, skeleton vibration, torsion molecule, and vibration of crystal lattice. The stretch mode of intramolecular heavy atoms can help to characterize the compounds that contain halogen atoms, compounds of organometallic and inorganic compounds.

2.3. ATR TECHNIQUE

Attenuated total reflection (ATR) is a technique for sampling without any further preparation (combined with IR) that enables to inspect the sample directly in either the solid or liquid state (Chan & Kazarian, 2016). However, the sampling technique used in the analysis depends on the form of sample and instrument. One of the major advantages of the IR spectroscopy is the use of ATR sampling technique that helps to obtain the spectra from several solid, liquid, and gas. However, it is necessary to prepare a sample in some cases to obtain a good quality spectrum. But ATR technique, over the years, bring a revolution for solid and liquid sample analysis because of its ability to handle the most difficult features of IR analyses particularly, the sample preparation and the reproducibility of spectra.

There are several key features of ATR sampling technique that are its ability for fast sampling and the ability of ATR to improve sample to sample reproducibility. Moreover, ATR sampling technique helps to minimize the user to user spectra variation and it has the capacity to produce high quality spectral database for more detailed verification of the material and its respective identification.

Attenuated total reflection technique operates when a beam comes into contact with a sample and resulting changes happening in an internally reflected infrared spectroscopy. At a certain angle, a high reflective index of an optically dense crystal being directed to an IR beam. Consequently, an evanescent wave is being created by intern reflectance which is extended beyond the crystal surface into the sample that is held in contact with the crystal (Kazarian & Chan, 2010).

The analysis of liquids and solids are followed by the cleanliness of the sample as soon as the crystal from the sample is cleaned, the liquid analysis collects the background of infrared. The necessary condition for a good analysis is to cover the whole crystal for qualitative or quantitative analysis. Moreover, to retain the sample, crystal must be settled into a metal plate, however, other semi-solid samples can easily be measured through scattering on a crystal. For the purpose of quantitative analysis, we use horizontal ATR units because of their ability to be easily cleaned and maintenance.

On the other hand, the analysis of the solids are usually examined using a single ATR accessory, for instance, the use of diamond is most common and preferred due to its resilience and heftiness. Before placing the solid material on the crystal area, the cleanliness of the crystal area

and the related background collection is a must. In the area of solid sample analysis, the previous researches and experience has depicted that the perfect results are achieved using powder sample and just placing enough sample to cover the crystal area. Moreover, it is important to note that the height of the sample must not be more than a few millimeters.

The ATR technique accessory function to measure the changes occurring in a total internal reflected IR beam in the context when sample and beam make a contact. The infrared beam has a direction towards optical thick crystal that contains a high refractive index at a particular angle. Therefore, it creates an internally reflectance evanescent wave extending beyond the crystal surface hooked on the respective sample. In order to successfully conduct the sample through ATR sampling technique, there are two major requirements to be fulfilled:

- It is necessary for the sample to directly make an interaction with the ATR crystal for the reason that bubble or passing wave extension is beyond the $0.5\mu - 5\mu$

- There must be a significant higher value for refractive index of the crystal compared to the value of sample or otherwise the occurrence of internal reflectance will not be possible the light will pass through instead of internal reflection in the crystal. Characteristically, the values of the refractive index ranges 2.38 And 4.01 at 2000 cm^{-1}, therefore, it is a safe assumption to state that most of the solids and liquids will have must lower refractive indices.

2.4. MOLECULAR VIBRATIONS

There are three different kinds of motion of molecules translational that is "when the whole molecule goes in the same direction", rotational state "when the molecule spins like a top", and the molecular vibrations (Woodward, 1972). Therefore, the molecular vibrational motion is one of these three kinds that happens when "the bonds between atoms within a molecule move".

Vibrational frequency is also called as periodic motion, and molecular vibration's typical frequencies fall with the 10^{13} to 10^{14} Hz this range of frequencies then correspond to wavenumbers of approx. 300 to 3000 cm^{-1} (Sathyanarayana, 2015). Moreover, beyond zero degrees Kelvin, all bonded atoms molecularly vibrate for example, six illustrations show the molecular vibrations below:

Symmetrical stretching	Asymmetrical stretching	Scissoring (Bending)
Rocking	Wagging	Twisting
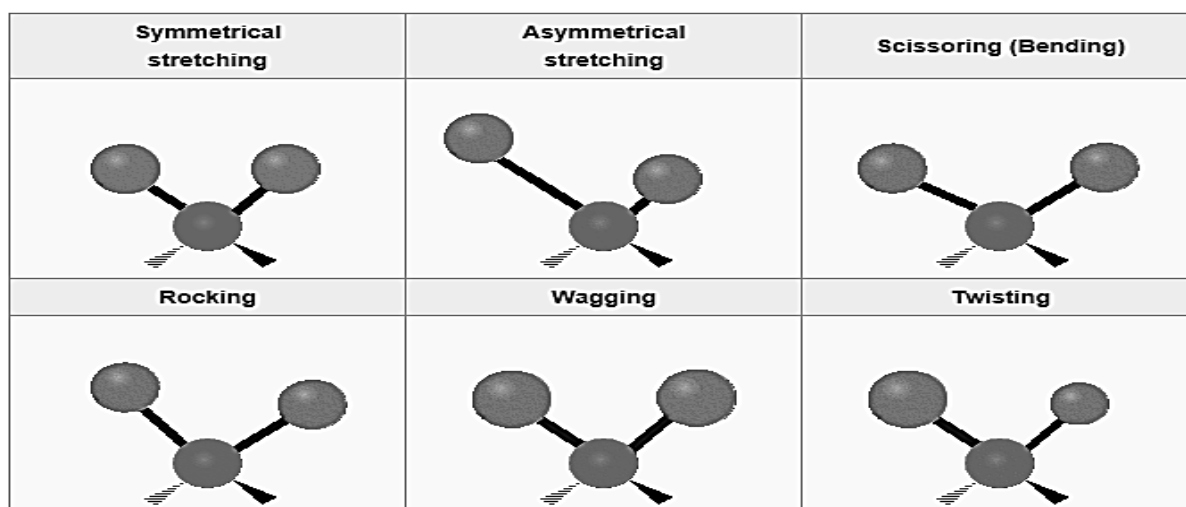
Figure 2.3: Molecule Vibration of a Methylene Group.

In the context of infrared spectroscopy, the main purpose is the identification of existing group functions in a particular particle. Infrared spectrometry analyzes the number of infrared photons and amount of energy originated within the infrared photons which are absorbed by the molecule.

A mirror or other such object that slowly turns, that only allows one frequency of IR light to pass through to the sample and reference detector at a time.

Source of IR light

Reference detector

An instrument that separates the different wavelengths of IR light. (Just as a prism separates white light into the colors of the rainbow).

Sample of unknown mixture

This detector detects photons that were not absorbed by the sample.

Figure 2.4: Simplified Infrared Spectrometer.

The given figure depicts how IR radiation is produced and separated into wavelengths of IR light, hitting a mirror and how it allows the particular wavelength of light, and then it reaches to a detector (Larkin, 2017). On the other hand, IR light directly reaches to the detector and one can measure the total IR light. Furthermore, the IR light passes through a sample and the photons of IR remained unabsorbed.

It is interesting to note when a sample of an unknown compound absorbs photons, the particular molecule advances energy a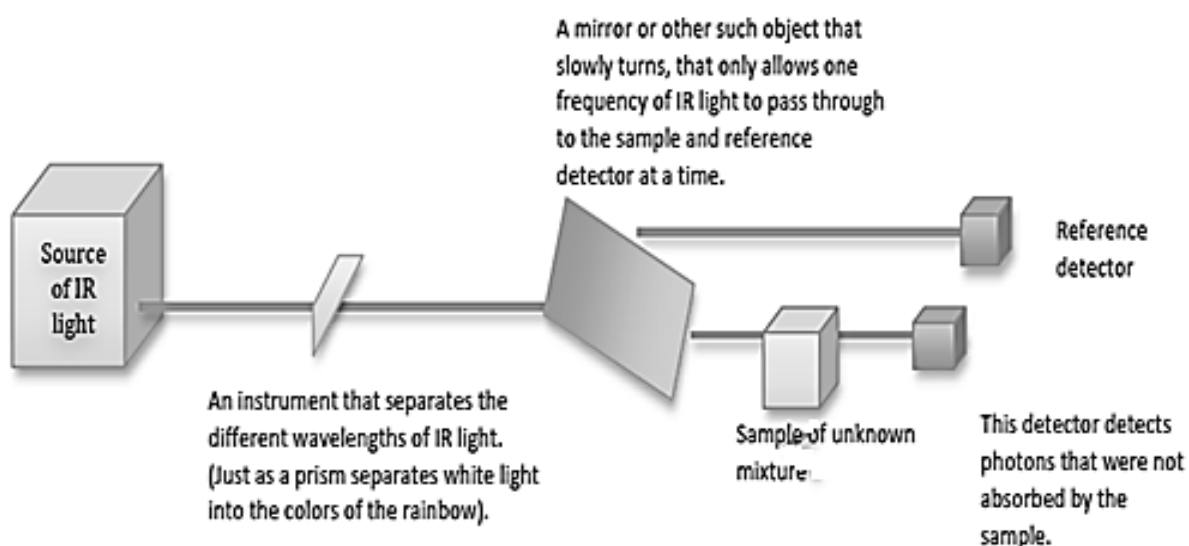nd moves from a lower state to a higher state of energy. Therefore, the lower energy state of vibration is called the "ground vibrational state", and the highest energy state of vibration is called the "exited vibrational state".

2.5. QUANTUM CHEMICAL CALCULATIONS

Quantum chemical calculations are based on quantum mechanics, and it contains the application of mathematical and theoretical principles to solve the chemical problems. Further, the researchers use quantum chemical calculations tool for the investigation of molecule structure, property, kinetic, and reactivity (Hehre, 2003). Moreover, these computational methods help chemists to conduct chemical phenomena using computers to study simulation in silico. It is also useful to examine the compounds and experience the reactions the calculations' results further help to predict the experiments and interpret the subsequent results.

Based on the fundamental laws of physics, the computational chemistry excites numerical chemical structures and reactions. However, in the current of era of technological innovation, computer programs help to perform quantum chemical calculations on molecules. The application of quantum chemical calculations has become a complementary aspect for investigations in organic, inorganic, physical chemistry, atomic physics, and molecular physics.

The computational chemistry mainly based on two broad areas of molecular mechanics and electronic structure. The basic type of calculations is as follows (Kaminski, Friesner, Tirado-Rives, & Jorgensen, 2001):

- Compute the energy of a specific molecular structure
- The optimization and performance of geometry that locates the lowest molecular structure

- It helps to compute the vibration frequency of particular molecule that results from inter-atomic motion. Atomic structure and frequency calculations helps to calculate the second derivative frequencies moreover, it can also predict the other properties. The calculations of frequencies are not possible for all "computational chemistry methods".

The laws of classical physics help molecular mechanics simulations to forecast the properties and structures of molecules there are several molecular methods available for that purpose. These molecular methods are considered on the basis of their force field. It is pertinent to note that the empirical results obtained through average of large number of molecules provide basis for "classical force field". These results are good for stranded systems because they are based on the widespread average of force fields however, one cannot use the force field generally for all molecules.

2.6. BORN-OPPENHEIMER APPROXIMATION

Born-Oppenheimer approximation (BO) assumes that quantum chemistry and molecular physics can separate the atomic nuclei motion and electrons in a particular molecule (Woolley & Sutcliffe, 1977). The term has been adopted from the names of the two scientists, who proposed the phenomena. The BO approach in terms of mathematics permits the fragmentation of electronic and nuclear in a wave-function of a particular molecule. These two components are also called vibrational and rotational. The equation is as follows:

$$\Psi_{total} = \psi_{electronic} \times \psi_{nuclear} \tag{2.1}$$

The approximation is used to simplify the energy calculation and the wave function of a molecule of an ordinary size for example, there are 12 centers in addition 42 electrons in a "benzene particle". Therefore, it is relevant to mention here that the "time independent Schrodinger equation" that helps toward the attainment of energy plus wave-function of a molecule it contains the 162 variables in a differential equation of eigenvalue and electrons with nuclei's spatial coordinates (Scherrer et al., 2017). Therefore, the Born-Oppenheimer approximation helps to calculate the wave-function in a process of two consecutive steps which are uncomplicated. The Born-Oppenheimer approach is essential in quantum chemistry since its initial proposal in 1927.

The two steps which are less complicated process of BO calculation is explained as the major phase to solve the "electronic Schrodinger equation" which helps to obtain the wave-function

$\psi_{electronic}$ that only depends on electrons. For example, if we take a case of "benzene" wave-function it depends on 126 electronic coordinates. On the other side, the "nuclei" is usually fixed in equilibrium configuration. The second step of Born-Oppenheimer approximation serves as the only nuclei in the Schrodinger equation and for the given benzene example it contains 36 variables (Min, Abedi, Kim, & Gross, 2014).

One of the major reasons for the success of the Born-Oppenheimer approximation is the differentiation of nuclear and electronic mass. In quantum chemistry, the Born-Oppenheimer is a significant tool because it handles large molecules of any wave-function and without the use of BO only light molecule can be handled e.g., H2. Therefore, the most important factor behind the success of Born-Oppenheimer approximation is its ability to differentiate the nuclear and the electronic mass.

2.7. BASIS SETS

The basic set of orbitals is always useful in the calculations of the AB initio electronic structure calculations. In order to get a perfect explanation for oscillator wave function, one has to set the large basic sets. Generally, the work of the foundation is focused on atoms and these are also called atomic orbitals (Roos, Lindh, & Malmqvist, 2016). Though, it is necessary to mention here that these atomic orbitals are not the solution of electromagnetic converter equator for the particular atom. In the contemporary process, it works based on the atom center; usually the type of Gaussian type orbitals (GTO) is selected which is stated as:

$$\Psi_{GTO}(x, y, z) = x^1 y^m z^n e^{-cr2} \tag{2.2}$$

The above given equation comprised of:

- *x, y, z*—that refer to the Cartesian coordinates of a local atom
- *l, m, n* refer to positive integers that describe the impetus of an orbital
- *r* refers to the circular space
- *l=m=n=0* depicts a spherical orbital
- *l=1 and m=n=0* refers to PX orbital
- *l=m=1 and n=0* is given by the orbital

It is pertinent to mention here that there are no radial nodes in the Gaussian-type orbitals (GTO's), unlike "hydrogen atom orbitals", though; it is possible to obtain the radial nodes by a combination of several different GTO's. Therefore:

- Fixed linear combination of GTO actually refers to the frequent function of atomic basis that is also called as contracted Gaussian function.

The minimal basis set refers to the least small conceivable basic set and it contains an orbit for each empty space including empty orbits, that is generally considered as an atom. For example, hydrogen has only one orbit, but on the other hand, carbon has five different orbits such as (1s, 2s, 2px, 2py, & 2pz). However, for carbon atom, there is an evacuation of p orbital.

Based on STO-3G that contracts three Gaussian functions which is a famous minimal basis set that is accurate but it is very difficult to calculate as well. Moreover, slater-type orbitals are a well-known minimum basic set that provides information on three Gaussian functions. A thin GTO can provide a decent estimation of a nuclear orbit, but it is not flexible to shrink or expand when there are other atoms exist in a particle. Therefore, at least one basic set, such as STO-3G, does not have the ability to produce extremely precise outcomes.

In order to describe each atom despite the availability of minimum numbers, one has to add additional basic functionality. Then, Hartree-Fock approach that will be described in the next section can make each atomic trajectory more or less weighted so that the wave function is better defined (Dyall, 2016). If at least two basic functions are at a minimum, this is called the base set "double zeta".

For this reason, a pair of zeta basins for hydrogen contains two different functions and carbon zeta bed is a true pair that contains the ten functions. Though, there are some instances when researchers deceive to use single trajectory for the given nucleus and produce nine functions for carbon and these functions refer to basic clusters which are also known as dual zeta in a valence field or basic sets of split valence (Schäfer, Huber, & Ahlrichs, 1994). Furthermore, these dual sets also refer to DZs. In general, the addition of basic functions that contains the highest angular momentum increases the flexibility. The orbital p describes the maximum kinetic momentum for carbon and the polarization of atom is defined using additional functions of d.

There are series of p functions which are used as functions of polarization for any hydrogen atom. Moreover, a series of DZPs helps to identify the dual zeta polarization basis. One of the

well-known examples of double fragmented polarization of dual zeta is 6-31G*. This indefinite notation refers to the valence of orbitals being described by two, the central orbit being defined as the narrowing of the Gaussian orbitals of 6 Gauss, one to three Gauss and the other a constriction of any single one function of Gaussian (Roos, Lindh, & Malmqvist, 2016). The use of asterisk (*) represents the function's polarization in any particular atom other than hydrogen. If the polarization is also added to the hydrogen atoms, this base is 6-31G**. The combined nature of the terminology is clearly listed in the polarity functions of 6-31G (d, s) that led some chemists to start to passing into slightly improved evaluation.

2.8. HARTREE-FOCK APPROACH

The Hartree-Fock (HF) approach is used in computational physics that determines the functions of wave and a multi-body energy of a quantum system in a motionless state (Slater, 1951). The Hartree-Fock approach helps us to measure the wave-function on the basis of several assumption, HF assumes that exact number of N-body functions of waves in a given system; the determinant of slater in the situation where molecules are fermions; or a single permanent calculation of a wave-function in a situation of N spine orbitals. However, on the other hand, one can invoke the "variational method" to estimate a set of equations for a number of orbitals. Therefore, the solutions to all these equations are helpful in the calculations of wave-functions and the value of energy in a given system.

The Hartree-Fock method usage increased rapidly with the advancement of the computers in 1960s despite the ability of the method to provide accurate and physical picture. Moreover, the usage of the method has been on rise since the advancement of the computer because of the computational demands on the empirical methods, particularly, the Hartree-Fock method. The initial application of the Hartree method and the Hartree-Fock approach is commonly applied to the analysis of the atoms because the system allows providing a simple picture of the problem.

The early literature states that "self-consistent filed method (SCF)" is the old name of the Hartree-Fock approach. Moreover, the approximate solution to the "Schrodinger equation" is basically now called the Hartree equation it requires the self-consistent distribution of charge that must associate the initial field and the final field (Umar, Oberacker, & Simenel, 2015). Therefore, it is concluded that the self-consistency is the basic requirement of the Hartree-Fock solution. The iterative method universally used to solve the equations; however, it is not

necessary for iteration algorithm to converge always. Therefore, the Hartree-Fock method is not always capable to solve the nonlinear equations.

2.8.1. Wave Function Approximation

It is pertinent to mention here that form of electron wave function and the assumption that Hartree-Fock approach makes is the basic key to this method. In order to perform the calculations, the basic assumption that method make is "*I* electron in orbit around a number of nuclei". The general form of the set of electron which a wave function describes is as follows:

$$\Psi(\vec{r}_1, S_{z1}, \vec{r}_2, S_{z2}, \dots \dots \dots \dots, \vec{r}_i, S_{zi}, \dots \vec{r}, S_{z1}) \tag{2.3}$$

The equation above is interpreted as:

- " $\vec{r}_i$ is the position of election number *I* "

- " S_z, it's spine in a chosen z-distribution "

- " the measurable values are $\frac{1}{2}\hbar$ and $-\frac{1}{2}\hbar$ "

Therefore, the answer of wave-function will depend on the nuclei, however, the positions of the nuclei has to be at their awarded positions that is because to reduce the clutter. Moreover, the positions of nuclear has not been explicitly shown that how they depend on the wave function of an electron.

The calculation of wave-function is based on the Hartree-Fock approach in the context where there is only one electron in a function (Kato, Ide, & Yamanouchi, 2015):

$$\psi_1^s(\vec{r}) \updownarrow_1 (S_z), \psi_2^s(\vec{r}) \updownarrow_2 (S_z), \psi_3^s(\vec{r}) \updownarrow_3 (S_z) \tag{2.4}$$

The equation is interpreted as:

- $\updownarrow$ depicts for any spin-up ↑ and spin-down ↓

- ↑ (s_z) would be equal to one if S_Z is $\frac{1}{2}\hbar$ "

- "Zero if it is $-\frac{1}{2}\hbar$ "

- " ↓ (s_z) equals zero if S_Z is $\frac{1}{2}\hbar$ and one if it is $-\frac{1}{2}\hbar$ Therefore, the given functions are "orbitals" and "spin orbitals".

The "orthonormal set" has been taken as the spin orbitals therefore, "two spin orbitals" are "automatically orthogonal" in case of contradictory rotations, for instance, the conditions of spine are "orthonormal $\langle \uparrow \mid \downarrow \rangle$ =0". However, the spatial orbitals will be orthogonal in case of the similar spine. Therefore, the single electron functions of products forms can be joined into to manifold functions of electron:

$$a_{n1,n2,\ldots n1}\psi_{n1}^{s}(\vec{r}) \updownarrow_{n1} (S_{z1})\psi_{n2}^{s}(\vec{r2}) \updownarrow_{n2} (S_{z2}) \ldots \psi_{n1}^{s}(\vec{r1}) \updownarrow_{n1} (S_{z1}) \tag{2.5}$$

- For electron 1, n1 represents the number of single electron function
- For electron 2, n2 refers to the number of single electron function "$a_{n1,n2,\ldots.n1}$ refers to the constant
- Therefore, Hartree product is derived from the given product wave function

The possibility for calculation of multi electron wave function depends on the high accuracy of arbitrarily if someone uses a single electron function with all their Hartree products (King, Baskerville, & Cox, 2018). Furthermore, it is important to note that even the most powerful computer systems are unable to solve the problems, thus, it is necessary to use the least. However, on the other hand, it is necessary not to use too few that will impose an "antisymmetrization requirement".

Therefore, the use of absolute the minimum possible is the basic condition for Hartree-Fock approximation as I electron represents the single electron function I. Therefore, Ψ can be used to represents the single determinant of Slatter.

$$\frac{a}{\sqrt{I}}\begin{pmatrix} \psi_1^s(\vec{r}_1)\updownarrow_1(S_{z1}) & \psi_2^s(\vec{r}_1)\updownarrow_2(S_{z1})\ldots\psi_n^s(\vec{r}_1)\updownarrow_n(S_{z1})\ldots & \psi_I^s(\vec{r}_1)\updownarrow_I(S_{z1}) \\ \psi_1^s(\vec{r}_2)\updownarrow_1(S_{z1}) & \psi_2^s(\vec{r}_2)\updownarrow_2(S_{z2})\ldots\psi_2^s(\vec{r}_2)\updownarrow_n(S_{z2})\ldots & \psi_I^s(\vec{r}_2)\updownarrow_I(S_{z2}) \\ \psi_1^s(\vec{r}_2)\updownarrow_1(S_{z1}) & \psi_2^s(\vec{r}_2)\updownarrow_2(S_{z2})\ldots\psi_n^s(\vec{r}_i)\updownarrow_n(S_{z2})\ldots & \psi_I^s(\vec{r}_i)\updownarrow_I(S_{zI}) \\ \psi_1^s(\vec{r}_I)\updownarrow_1(S_{zI}) & \psi_2^s(\vec{r}_I)\updownarrow_2(S_{zI})\ldots\psi_n^s(\vec{r}_I)\updownarrow_n(S_{zI}) \ldots & \psi_I^s(\vec{r}_I)\updownarrow_I(S_{zI}) \end{pmatrix} \tag{2.6}$$

- **a** represents the constant
- Sum of I is equal to the determinant of slater
- I single electron helps to derive the single wave function
- Any two of the I electrons when exchange refers to antisymmetric

$$\Psi = \frac{a}{\sqrt{I!}} \downarrow det(\psi_1^s \updownarrow_1, (\psi_2^s \updownarrow_2, \ldots., \psi_n^s \updownarrow_n, \ldots., \psi_I^s \updownarrow_I \tag{2.7}$$

It is important to note that the use of minimum number for functions of single electron will definitely produce an error and if we mathematically consider this error, it is not small. Therefore, the use of several different numbers for determinants of Slater could only produce an neglectable small error. However, Hartree-Fork approach still generates good results that can satisfy the requirements of the users and it is possible to improve the results with the use of Post Hartree-Fock methods.

2.8.2. Algorithm Flowchart

The energy produced through Hartree-Fock's provides a limit that is beyond the actual energy produced in a given molecule. Moreover, the Hartree-Fock method provides the best solution to limit the energy when the base of the approach reaches to the completion (Qiu, Henderson, & Scuseria, 2017). Furthermore, it is necessary to mention here that the previous two approximations of the Hartree-Fock theory that were explained earlier, are cancelled and C1 is referred to a complete limit. The exact solution can only be obtained when both limits reached to approximation of the Born-Oppenheimer, and the energy produced through Hartree-Fock would be the minimum of any single determinant of Slater.
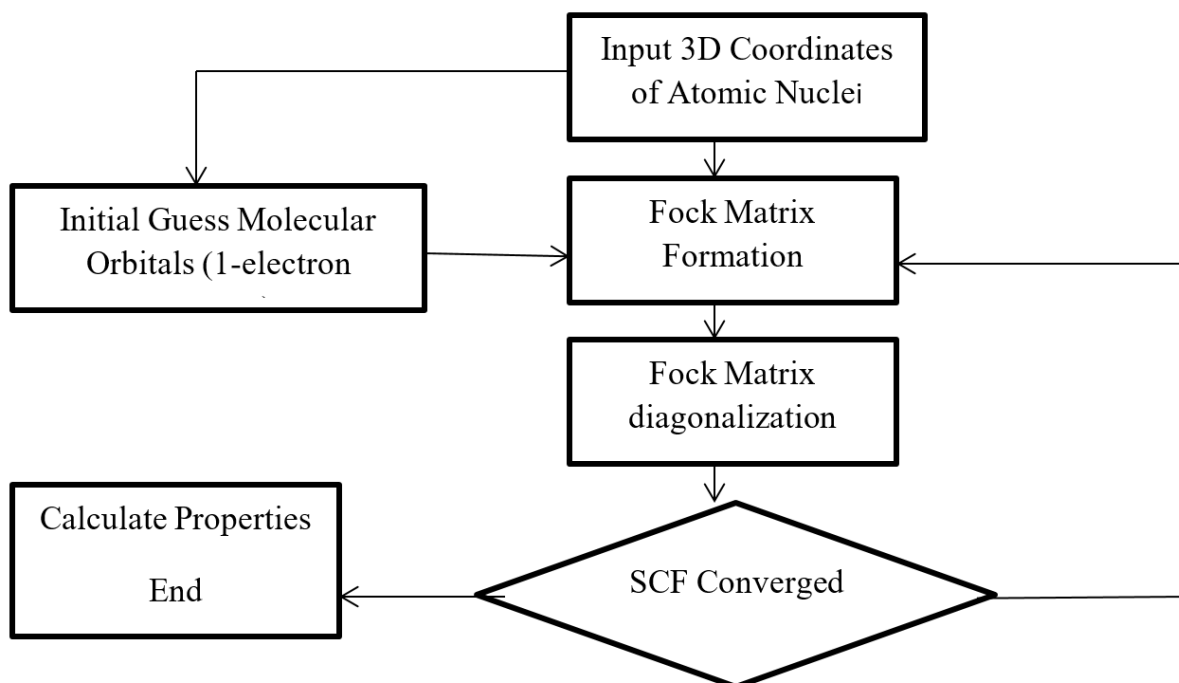
Figure 2.5: Algorithmic flowchart of Hartree-Fock.

2.8.3. Approximations

In order to deal with it there are five simplifications which are made through Hartree-Fock approach (Umar, Oberacker, & Simenel, 2015):

- There is an inherent assumption for Born-Oppenheimer approximation
- The impacts of the relativism are completely ignored, and there is an assumption that momentum operator has to be fully non-relativistic
- There is an assumption regarding the variational solutions that basic functions of finite numbers provide the linear combinations
- A single determinant of Slater is assumed to describe every energy eigenfunction and it is an anti-symmetrized product of non-electron wave function
- There is an assumption to neglect the deviations and their effects that arise from the implication of the approximation of mean field. The electron correlation is defined through these collective effects

2.9. DENSITY FUNCTIONAL THEORY

The theory of Density Functional (DFT) refers to a method of computational that is used in the quantum modeling in physics, chemistry, and material science that help to study the structures of electron of several bodily systems particularly, the study of atom, molecule and its phases, and the phases of condensed (Koch & Holthausen, 2015). The theory helps to determine properties of several systems of electrons using functional functions of any other function that the density of electrons depending on the space. Hence, the functional density of the name density results from the use of functional electron density. The application of the Density functional theory is considered prevalent in condensed matter physics, computational physics, and computational chemistry.

Since 1970s, density functional theory remained an important method of approximation in solid-state physics however until 1990s, this method was well-thought-out inaccurate for calculations in quantum chemistry although, there have been some refinements made to this theory to make it useful for exchange and correlation interactions. Unlike the other old-style methods i.e. Hartree-Fock theory and other successors (electron correlation), the computational costs are much lesser in density functional theory (Jones, 2015).

It is pertinent to note that despite the refinements and respective improvements in the theory there exists several difficulties to describe:

- The interactions of inter-molecule that is important to understand the chemical reactions
- There is difficulty existing to measure the van der Waals forces
- The excitations of charge transfer
- The states of transition
- The surfaces of potential global energy
- The interactions of dopant
- The systems of correlation
- The approximation of gap of band and semiconductor's ferromagnetism

The accuracy of the density functional theory has been greatly damaged the treatment of dispersion and the other systems that are dominated by dispersion.

Ab initio, the density functional theory calculations, in the context of "computational materials science", permit to predict and calculate the material behavior on the basis of "quantum mechanical considerations" these predictions and calculations do not require high order parameters e.g. fundamental material properties. In the modern techniques of density functional theory, the evaluation of structure of electron is based on the potential acting on electrons of a system (Koch & Holthausen, 2015).

2.9.1 Hohenberg And Kohn

It is important to note that calculations for many-body electronic contain fixed nuclei in the treated molecules and clusters for instance, the approximation of Born-Oppenheimer where electronic move and that generate a motionless peripheral potential V (Medvedev et al., 2017).

- 1st Hohenberg-Kohn Theorem where electronic density n(x,y,z) is the only dependent upon which several ground state properties of numerous electron systems depend
- 2nd Hohenberg-Kohn Theorem: The function of E[n(x,y,z)] helps to minimize the total energy for a true ground state density of a system

$$E_{GS} \equiv ground\ state\ energy$$

$$\phi_{GS} \equiv non-degenerate\ ground\ state\ N-electron wave\ function$$

$$H\phi_{GS} = E_{GS}\phi_{GS}$$

$$\phi_{GS}$$

$$V_{ext}$$

$$p_{GS}(r) = \sum_{OCC} \phi_{GS}(r)^2$$

$$one-to-one$$

$$p_{GS}$$
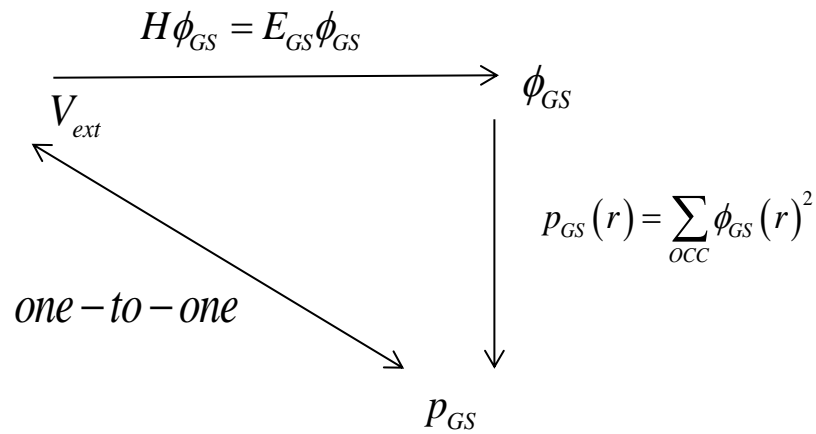
$$p_{GS} \Rightarrow V_{ext} \Rightarrow H \Rightarrow \phi[p_{GS}] \Rightarrow o[p_{GS}]O\phi[p_{GS}]O\phi[p_{GS}]$$

$$p_{GS}(x,y,z) \text{ and not } \phi_{GS}(x_1,y_1,z_1,\ldots.x_N,y_N,z_N) \text{ is the basic variable}$$

2.9.2. Applications

Generally, the density functional theory is applied to the chemical and material sciences in order to get the interpretation and predictions of complex systems and their behavior at an atomic scale. Particularly, density functional theory compute approaches apply to study the systems to synthesis and process parameters. The modern applications of the density functional theory are, for example (Jones, 2015):

- It helps to study the dopants effects on the transformation phase of behaviors in oxides
- The study of magnetic and the behavior of magnetic in dilute magnetic semiconductor materials
- The dilution of magnetic semiconductors and their electronic behaviors
- It helps to predict the sensitivity of few nanostructures e.g., the SO2 or Acrolein as environment pollutants
- "The prediction of mechanical properties"

Practically, the "Kohn-Sham Theory" has a wide range of application in multiple scenarios; however, the application is solely depends on what is needed to be examined. The solid state approximations, the most common estimation of local density coupled with the basis sets of wave and electron gas approach is far better for delocalized electron within an infinite solid (Perdew et al., 2017). Moreover:

- There are requirement for the sophisticated function to calculate the of molecule and there has been several varieties of exchange correlation for chemical applications
- There is an inconsistency between the approximation of uniform electron gas, although, the electron gas limit must be reduced to LDA
- Perdew-Burke-Ernzerhof exchange model has been the widely used functional among physicists, although, the accuracy of calorimetrical is not sufficient in the calculations of molecule gas-phase
- BLYP is an extensively used function for the researchers
- "B3LYP hybrid function is even widely used for energy exchange and there is a combination of Hartreee-Fock theory and the Becke exchange function

2.10. NORMAL COORDINATE ANALYSIS

The normal coordinate analysis is used in the calculations of frequencies of normal modes of vibrations in terms of suitable coordinates the normal coordinate analysis is based on "a classical mechanics approach using harmonic approximation" (Jensen, 2017). The main purposes of the normal coordinate analysis are as follows:

- "to calculate the vibrational frequencies and their assignments to support the qualitative interpretation of spectra"
- "to discuss the reliability of the information including the force constants obtain form the computation"

A thorough analysis of the normal coordinates produce a vibrational quantitative description of motion for all atoms in the context of force constants that define each bond's resistance which stretches and bends the vibrations. It is pertinent to mention here that normal coordinate analysis with the help of modern computer programs and available correct vibrational spectra has gained a significant success in a application of bigger molecules.

2.10.1. Normal Coordinate Analysis Procedure

For a better understanding of the application of the normal coordinate analysis, a stepwise outline is given below (Wollrab, 2016):

Step 1

Before the application of the normal coordinate analysis, there are certain assumptions that have to be met before performing the analysis. For instance:

- One should know the structure of the molecule before performing normal coordinate analysis.
- If the first condition is not fulfilled, and the structure of the molecule is unknown, then the "structure would be assumed and bond lengths with bond angles were transferred from related molecules".

Furthermore, the data used for normal coordinate analysis can be obtained "X-ray structure determination" or "micro wave spectra".

Step 2

In order to perform the normal coordinate analysis, the modes for vibration such as "stretching, blending, torsion, and out of plane bending are determined for the molecular model".

Step 3

The irreducible representations of the point group are used to classify the normal modes of polyatomic molecules this is where the molecules belong.

2.11. INTERNAL COORDINATES

In the context of normal vibrations, the status of vibrational coordinates change in the positions of atoms in the molecule after the excitement of the vibration and respective sinusoidal changes in the coordinate with a certain frequency V and the vibrational frequency (Sittel, Jain, & Stock, 2014). Therefore, the "internal coordinates" are illustrated below refereeing to the "planar molecule ethylene", and has following types:

$$H_2C=CH_2$$
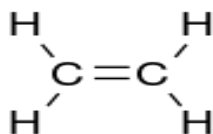
- Stretching refers to the length changes in a bond

- Bending refers to the change in the two bonds

- Rocking refers to the changes in the angle between atoms group

- Wagging is an angle change among the atoms group

- Twisting is an angle change amid two groups of atoms and the planes

- Out of plane is angle change amongst the bonds (C-H) and the respective plane that define the reaming atoms

There is no change involved in the lengths of the bonds with the groups in the context of rocking, wagging, and twisting coordinates but the angles do change. The differentiation between rocking and wagging is that rocking contains the same atoms in the group in the same plane. Moreover, the calculation for ethene regarding coordinates states that there are twelve internal coordinates, four stretching of C-H, one stretching for C-C, two bending for H-C, two rocking CH2, two wagging CH2, and one twisting (Baiardi, Bloino, & Barone, 2016).

Furthermore, it is noted that the "atoms in a CH2 group" vibrate in six different ways as the illustration below depicts.

2.11.1. Symmetry-Adapted Coordinates

The symmetry adapted coordinates are generated through the application of a projection operator that helps to set the internal coordinates and projection operator constructs the character table for molecular point group. For instance, the un-normalized four coordinates C-H stretching of the molecule ethane are $QS_1 = q_1 + q_2 + q_3 + q_4$, $QS_1 = q_1 + q_2 - q_3 - q_4$, $QS_1 = q_1 - q_2 + q_3 - q_4$ and $QS_1 = q_1 - q_2 - q_3 + q_4$.

In the above given coordinates, the stretching internal coordinates for four C-H bonds are q1-q4.

2.12. NORMAL COORDINATES

Q is usually denoted with the normal coordinates that normal mode of vibration which describes the equilibrium positions of the atoms positions are away from each other. It is important to mention here that each normal coordinate has one normal mode, and therefore, each normal coordinate denotes to the "progress" in line with the normal mode at any given point. In a very formal way, the solution of a secular determinant derived from normal modes, and then the description of normal coordinates with normal modes is expressed as summation over the Cartesian coordinates upon the positions of atoms.

There are several advantages of normal modes study that includes the diagonalization of the matrix that govern the vibrations of molecule, thus, there is an independent vibration associated with every molecule and each normal mode that associates with own spectrum of quantum mechanical state. Furthermore, the other conditions are as follows:

- A symmetric molecule will definitely belong to a point group that helps to transform the normal modes to irreducible representation under the respective group

- The qualitative application of group theory will determine the normal modes and project the complex picture on the Cartesian coordinates

For instance, if there is a treatment application to CO2, the results suggest that C-O stretching coordinates are not autonomous, in fact, the existence of a symmetric stretch O=C=O and asymmetric stretch O=C=O.

- Symmetric stretch refers to the sum of two stretch coordinates C - O, the changes in the bond lengths is equal to two bonds C - O, and the carbon atom is the stationary ($Q = q_{1} + q_{2}$).

- Asymmetric stretch states the changes of stretch coordinates C - O, as compared to the symmetric stretch bond length of C - O bond will increase while the other decrease ($Q = q_{1} - q_{2}$).

3. RESULTS

Experimental wavenumbers and wavenumber values calculated for the most stable structure of ETH are given in Table3.6. Optimized geometry parameters of ETH molecule and ETH-H_2O complexes are given in Table 3.1-3.5. Free energy of ETH molecule is found to be -818.607712487 a.u. Energy values of possible water complexes are found as -895.027888958 a.u., -895.028096376 a.u., -971.467567932 a.u and -895.034306954 a.u. respectively. Energy values of water complexes of ETH molecule are found lower than free ETH molecule and this fact shows us that water complexes are more stable than the free molecule.
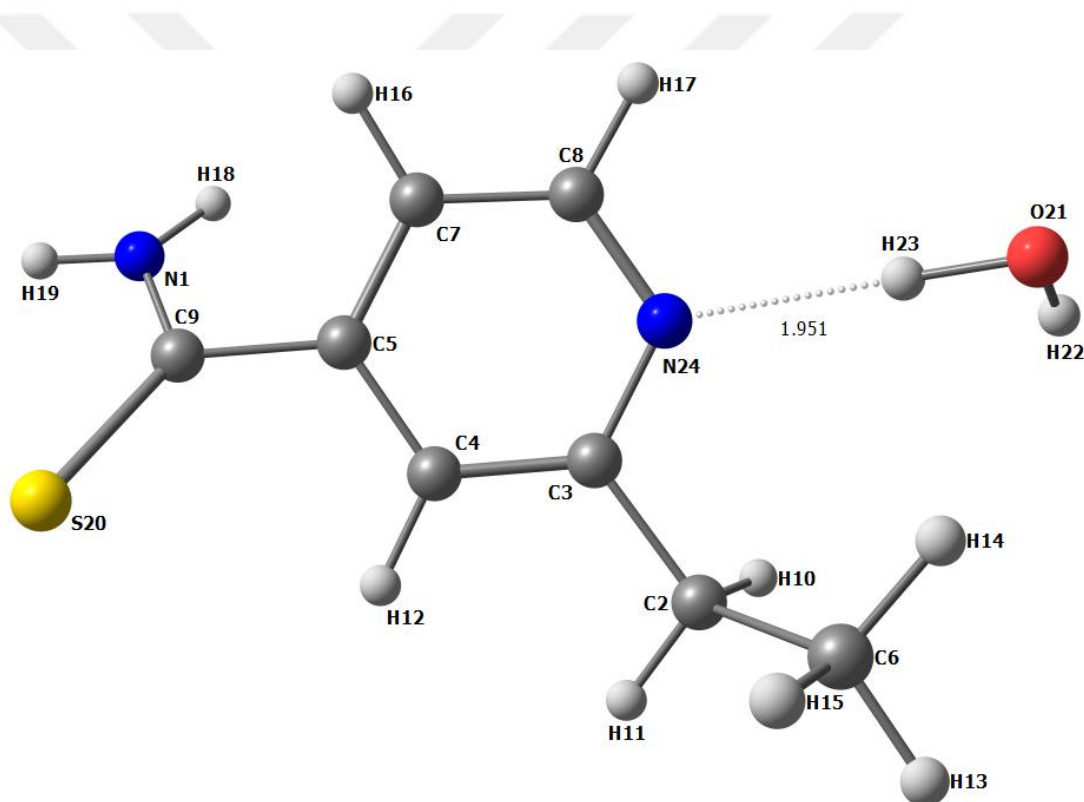

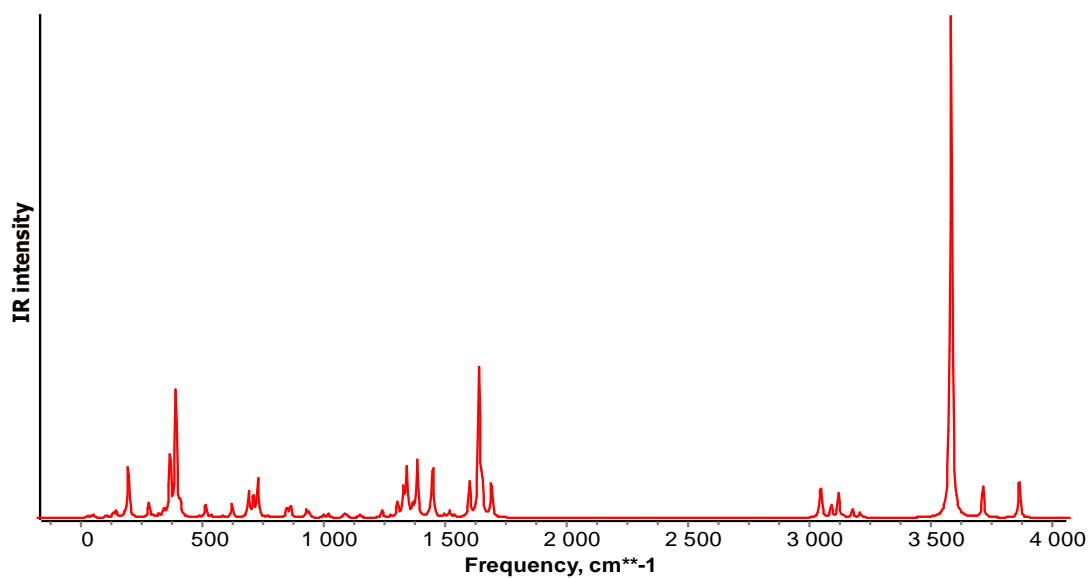**Figure 3.1:** Optmized geometry of ETH-water complex1.

Figure 3.2: Calculated IR spectra of ETH-water complex1.

Table 3.1: Calculated geometry parameters of ETH-water complex1.

Bond Distances(Å)

R(1-9)	1.351	R(5-9)	1.495
R(1-18)	1.009	R(6-13)	1.095
R(1-19)	1.010	R(6-14)	1.093
R(2-3)	1.512	R(6-15)	1.095
R(2-6)	1.539	R(7-8)	1.393
R(2-10)	1.097	R(7-16)	1.085
R(2-11)	1.095	R(8-17)	1.088
R(3-4)	1.398	R(8-24)	1.336
R(3-24)	1.348	R(9-20)	1.664

Table 3.1 (continued): Calculated geometry parameters of ETH-water complex1.

R(4-5)	1.399	R(21-22)	0.965
R(4-12)	1.084	R(21-23)	0.978
R(5-7)	1.402	R(23-24)	1.951
Bond Angles(^{o})			
A(9-1-18)	121.5	A(3-24-8)	118.6
A(9-1-19)	118.3	A(3-24-23)	124.8
A(1-9-5)	114.7	A(5-4-12)	119.3
A(1-9-20)	122.3	A(4-5-7)	117.8
A(18-1-19)	118.6	A(4-5-9)	120.7
A(3-2-6)	113.2	A(7-5-9)	121.5
A(3-2-10)	108.2	A(5-7-8)	118.5
A(3-2-11)	109.0	A(5-7-16)	121.6
A2-3-4)	121.6	A(5-9-20)	123.0
A(2-3-24)	117.0	A(13-6-14)	108.4
A(6-2-10)	109.1	A(13-6-15)	107.9
A(6-2-11)	110.3	A(14-6-15)	108.6
A(2-6-13)	110.1	A(8-7-16)	119.9
A(2-6-14)	110.7	A(7-8-17)	120.4
A(2-6-15)	111.0	A(7-8-24)	123.6

Table 3.1 (continued): Calculated geometry parameters of ETH-water complex1.

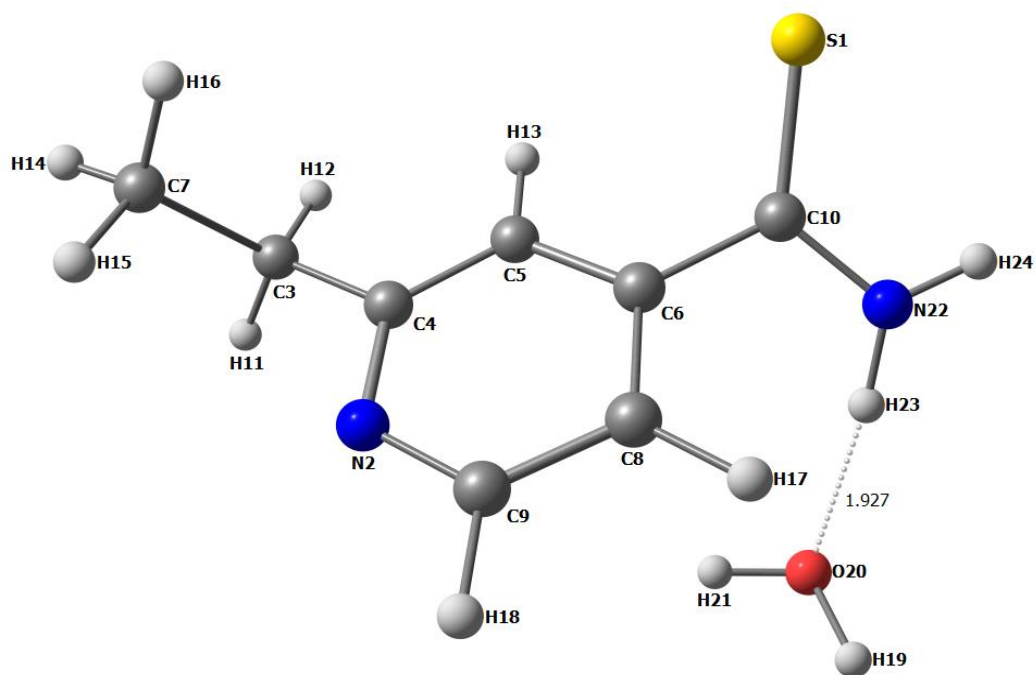| A(10-2-11) | 106.8 | A(17-8-24) | 116.1 |
A(4-3-24)	121.5	A(8-24-23)	115.1
A(3-4-5)	120.0	A(22-21-23)	103.7
A(3-4-12)	120.6	A(21-23-24)	174.0

A: Bond angle, R: Bond distance.

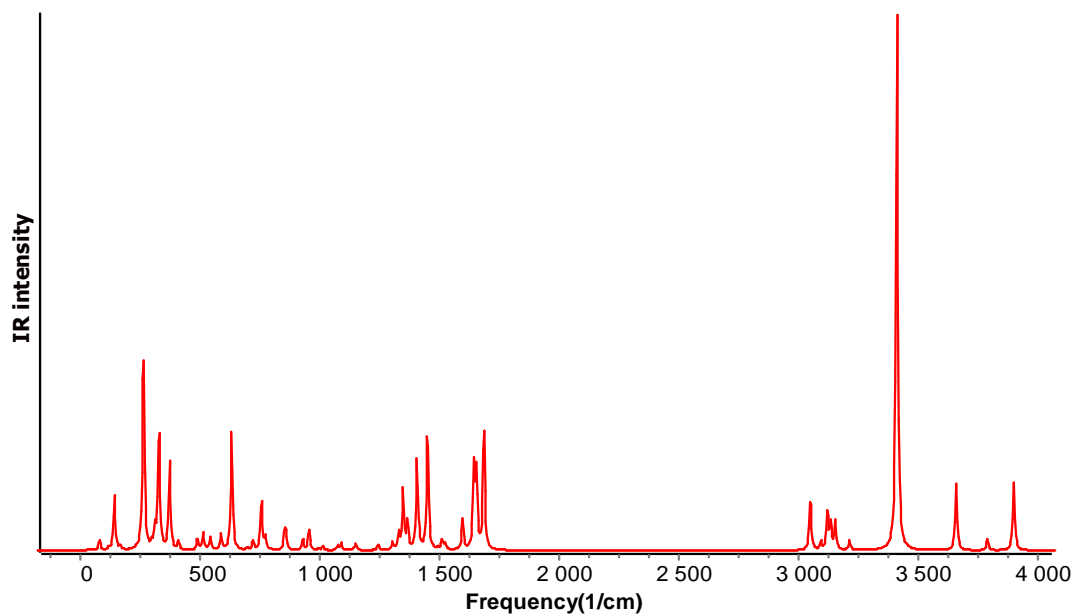**Figure 3.3:** Optmized geometry of ETH-water complex2.

Figure 3.4: Calculated IR spectra of ETH-water complex2.

Table 3.2: Calculated geometry parameters of ETH-water complex2.

Bond Distances(Å)

R(1-10)	1.670	R(7-14)	1.094
R(2-4)	1.347	R(7-15)	1.093
R(2-9)	1.336	R(7-16)	1.095
R(3-4)	1.512	R(8-9)	1.395
R(3-7)	1.538	R(8-17)	1.084
R(3-11)	1.096	R(9-18)	1.089
R(3-12)	1.095	R(10-22)	1.345
R(4-5)	1.399	R(19-20)	0.966
R(5-6)	1.398	R(20-21)	0.967
R(5-13)	1.084	R(22-23)	1.022
R(6-8)	1.403	R(22-24)	1.010
R(6-10)	1.496	R(20-23)	1.927

Bond Angles(°)

A(1-10-6)	122.0	A(6-5-13)	119.3
A(1-10-22)	123.2	A(5-6-8)	117.6
A(2-4-5)	122.2	A(6-8-9)	118.5
A(2-9-8)	124.0	A(6-8-17)	121.0
A(2-9-18)	116.0	A(6-10-22)	114.8

Table 3.2 (continued): Calculated geometry parameters of ETH-water complex2.

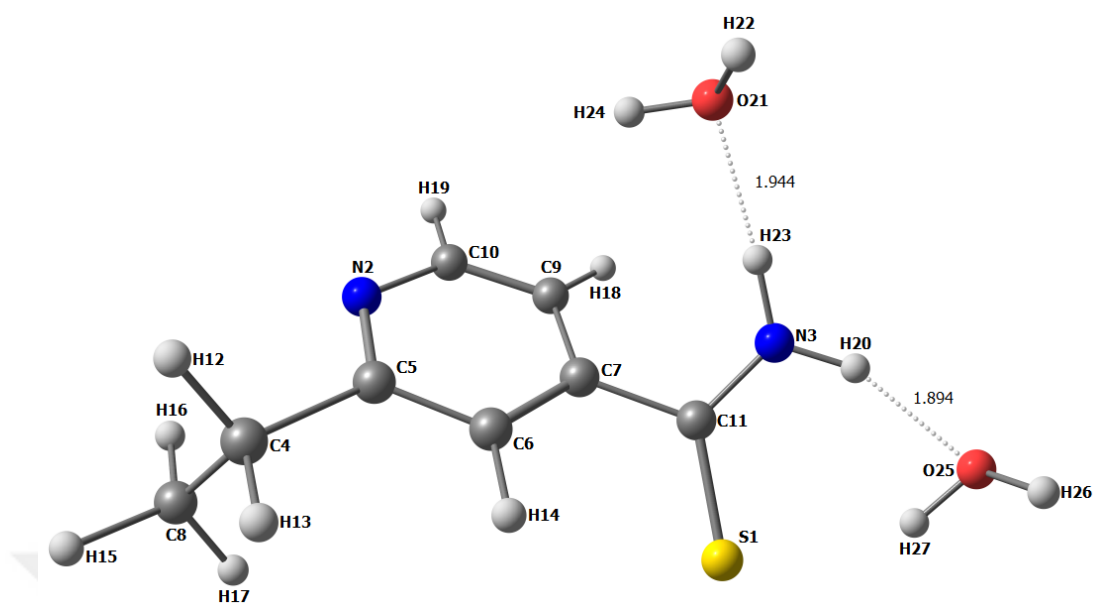|			
A(4-3-7)	112.3	A(14-7-15)	108.4
A(4-3-11)	108.2	A(14-7-16)	108.1
A(4-3-12)	109.6	A(15-7-16)	108.1
A(3-4-5)	121.6	A(9-8-17)	120.5
A(7-3-11)	109.1	A(8-9-18)	120.0
A(7-3-12)	110.1	A(10-22-23)	122.3
A(3-7-14)	110.8	A(10-22-24)	117.0
A(3-7-15)	110.2	A(19-20-21)	104.7
A(3-7-16)	111.1	A(19-20-23)	117.6
A(11-3-12)	107.4	A(21-20-23)	101.0
A(4-5-6)	119.9	A(23-22-24)	118.6
A(4-5-13)	120.8	A(22-23-20)	173.6

A: Bond angle, R: Bond distance.

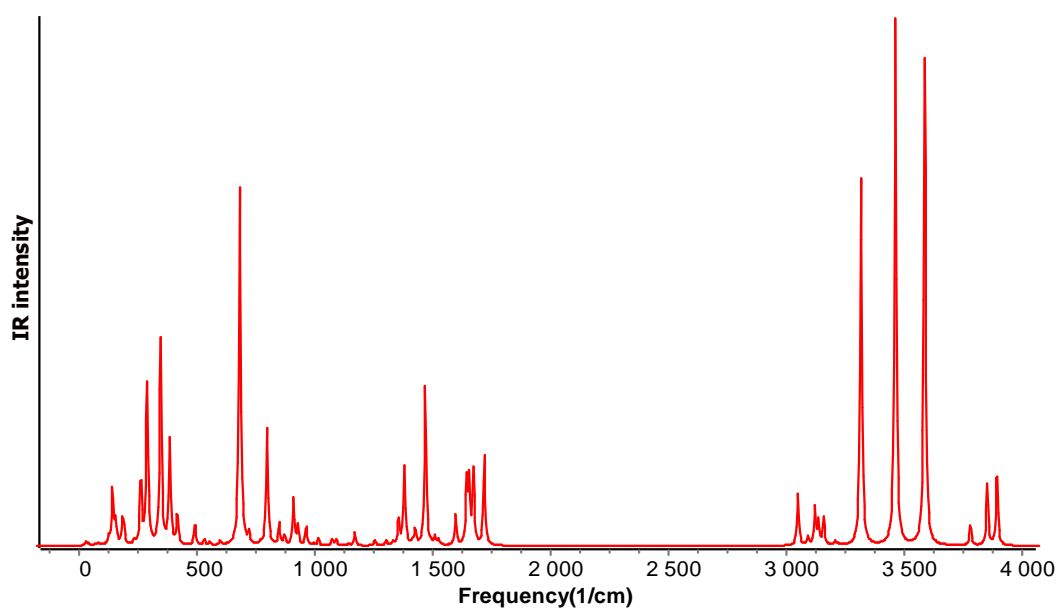**Figure 3.5:** Optmized geometry of ETH-water complex3.

Figure 3.6: Calculated IR spectra of ETH-water complex3.

Table 3.3: Calculated geometry parameters of ETH-water complex3.

Bond Distances(Å)

R(1-11)	1.687	R(7-11)	1.497
R(2-5)	1.346	R(8-15)	1.094
R(2-10)	1.336	R(8-16)	1.093
R(3-11)	1.333	R(8-17)	1.095
R(3-20)	1.026	R(9-10)	1.395
R(3-23)	1.022	R(9-18)	1.085
R(4-5)	1.512	R(10-19)	1.089
R(4-8)	1.538	R(21-22)	0.966
R(4-12)	1.096	R(21-24)	0.968
R(4-13)	1.095	R(25-26)	0.967
R(5-6)	1.400	R(25-27)	0.980
R(6-7)	1.398	R(20-25)	1.894
R(6-14)	1.084	R(21-23)	1.944
R(7-9)	1.403		

Bond Angles(°)

A(1-11-3)	124.1	A(4-8-17)	111.1
A(1-11-7)	120.3	A(12-4-13)	107.3
A(5-2-10)	117.9	A(5-6-7)	119.8

Table 3.3 (continued): Calculated geometry parameters of ETH-water complex3.

A(2-5-4)	116.2	A(5-6-14)	120.7
A(2-5-6)	122.2	A(7-6-14)	119.5
A(2-10-9)	124.0	A(6-7-9)	117.7
A(2-10-19)	116.1	A(6-7-11)	121.3
A(11-3-20)	118.4	A(9-7-11)	121.0
A(11-3-23)	121.2	A(7-9-10)	118.4
A(3-11-7)	115.5	A(7-9-18)	121.0
A(20-3-23)	120.0	A(15-8-16)	108.5
A(3-20-25)	157.4	A(15-8-17)	108.1
A(3-23-21)	171.1	A(16-8-17)	108.1
A(5-4-8)	112.3	A(10-9-18)	120.5
A(5-4-12)	108.2	A(9-10-19)	119.9
A(5-4-13)	109.6	A(22-21-24)	104.7
A(4-5-6)	121.5	A(22-21-23)	110.5
A(8-4-12)	109.1	A(24-21-23)	100.1
A(8-4-13)	110.1	A(26-25-27)	103.4
A(4-8-15)	110.7	A(26-25-20)	109.3
A(4-8-16)	110.2	A(27-25-20)	82.8

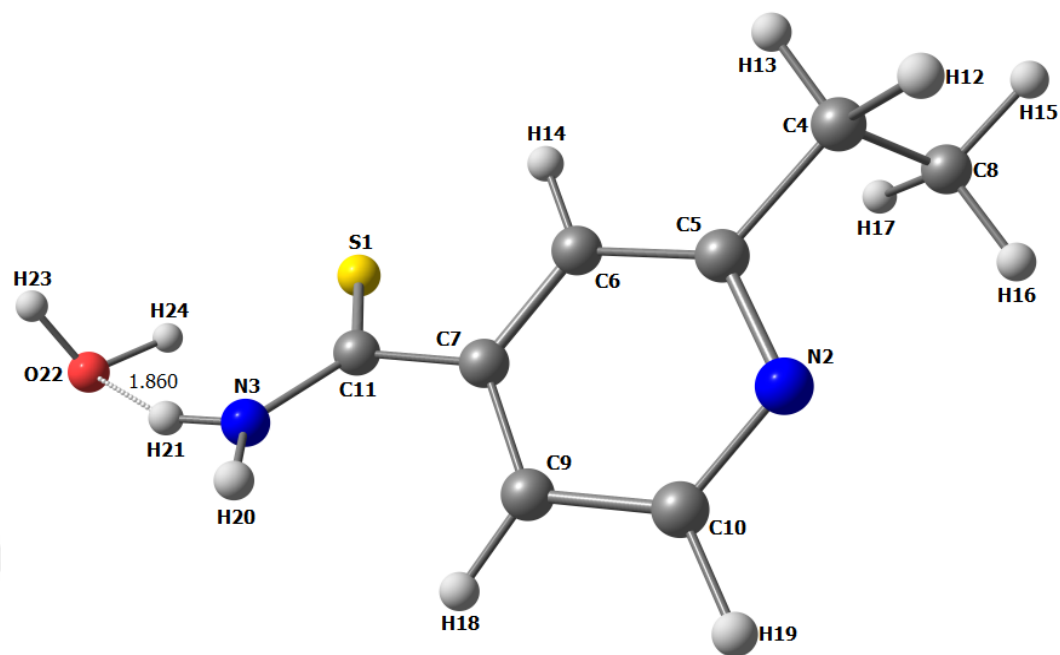A: Bond angle, R: Bond distance.

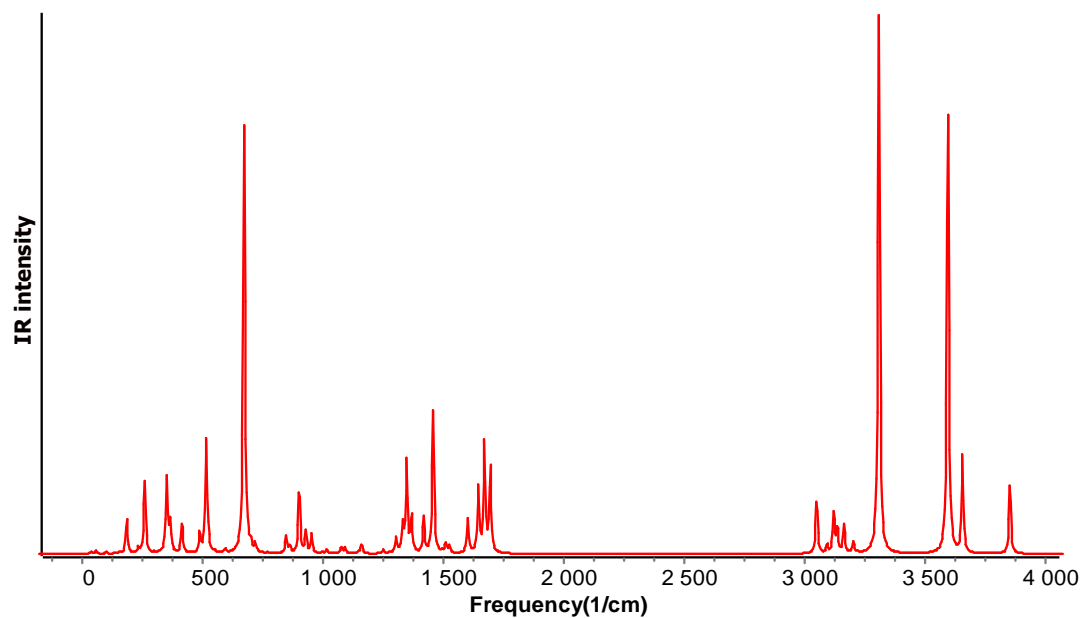**Figure 3.7:** Optmized geometry of ETH-water complex4.

Figure 3.8: Calculated IR spectra of ETH-water complex4.

Table 3.4: Calculated geometry parameters of ETH-water complex4.

Bond Distances(Å)

R(1-11)	1.683	R(6-14)	1.084
R(2-5)	1.347	R(7-9)	1.401
R(2-10)	1.335	R(7-11)	1.494
R(3-11)	1.338	R(8-15)	1.094
R(3-20)	1.010	R(8-16)	1.093
R(3-21)	1.028	R(8-17)	1.095
R(4-5)	1.512	R(9-10)	1.395
R(4-8)	1.538	R(9-18)	1.085
R(4-12)	1.096	R(10-19)	1.089
R(4-13)	1.095	R(22-23)	0.967
R(5-6)	1.398	R(22-24)	0.979
R(6-7)	1.399	R(21-22)	1.860

Bond Angles(º)

A(1-11-3)	122.9	A(4-8-16)	110.2
A(1-11-7)	121.5	A(4-8-17)	111.1
A(5-2-10)	117.9	A(12-4-13)	107.3
A(2-5-4)	116.2	A(5-6-7)	119.8
A(2-5-6)	122.2	A(5-6-14)	120.8

Table 3.4 (continued): Calculated geometry parameters of ETH-water complex4.

A(2-10-9)	124.0	A(7-6-14)	119.5
A(2-10-19)	116.2	A(6-7-9)	117.7
A(11-3-20)	120.3	A(6-7-11)	121.0
A(11-3-21)	119.5	A(9-7-11)	121.3
A(3-11-7)	115.6	A(7-9-10)	118.5
A(20-3-21)	119.9	A(7-9-18)	121.5
A(3-21-22)	157.8	A(15-8-16)	108.4
A(5-4-8)	112.3	A(15-8-17)	108.1
A(5-4-12)	108.2	A(16-8-17)	108.1
A(5-4-13)	109.6	A(10-9-18)	119.9
A(4-5-6)	121.6	A(9-10-19)	119.9
A(8-4-12)	109.1	A(23-22-24)	103.6
A(8-4-13)	110.1	A(23-22-21)	110.0
A(4-8-15)	110.8	A(24-22-21)	83.9

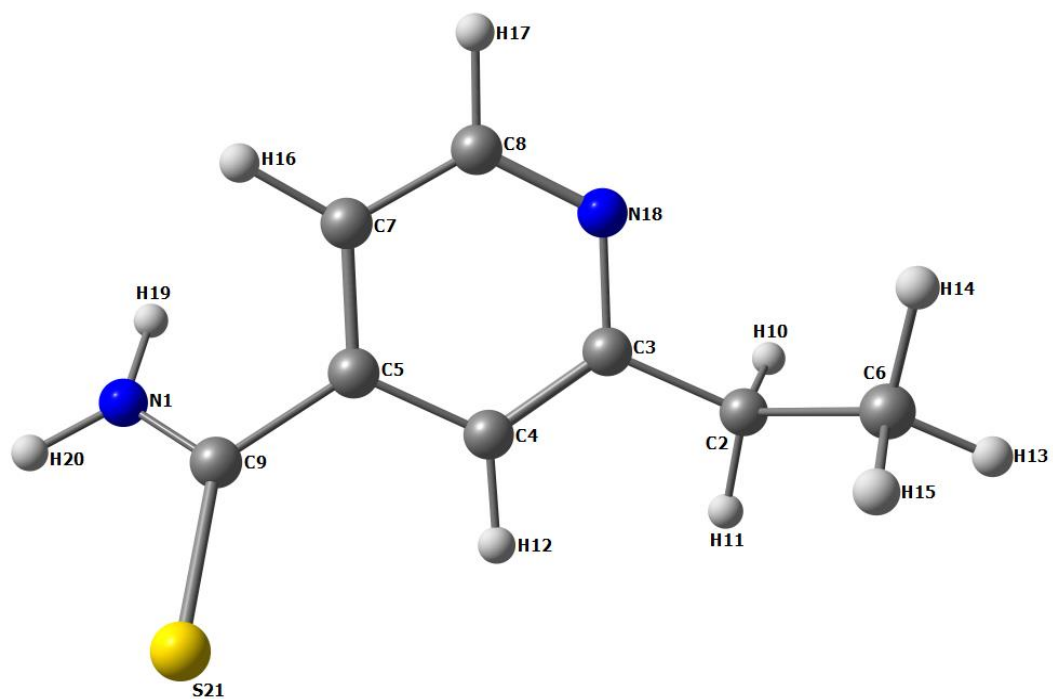A: Bond angle, R: Bond distance.
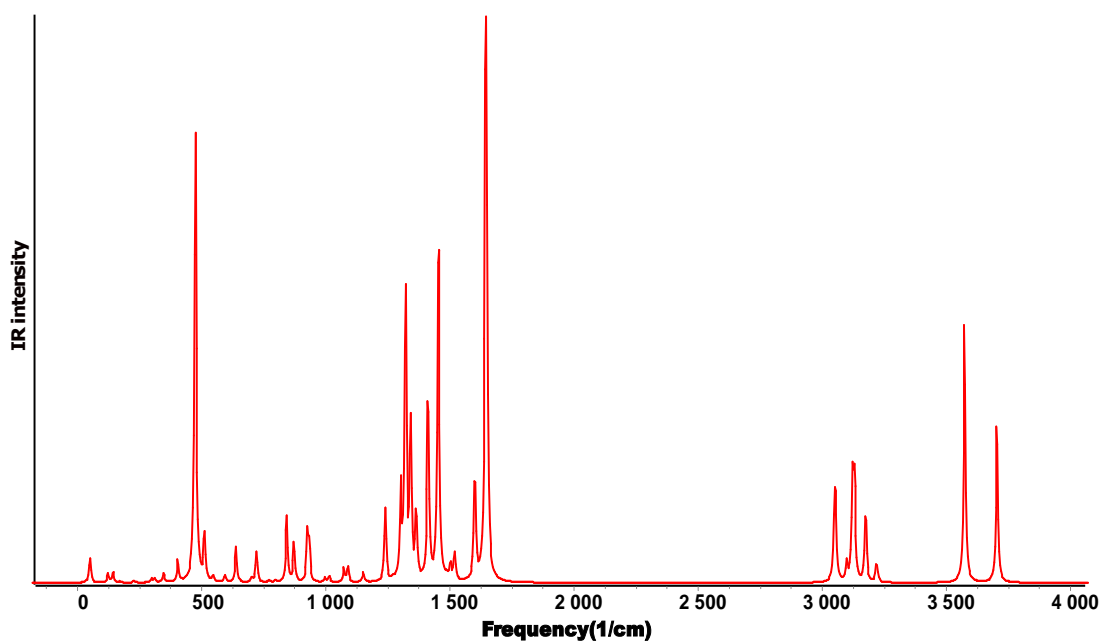
Figure 3.9: Optmized geometry of ETH.

Figure 3.10: Calculated IR spectra of ETH.

Table 3.5: Calculated geometry parameters of ETH.

Bond Distances(Å)

R(1-9)	1.334	R(5-7)	1.401
R(1-19)	1.011	R(5-9)	1.494
R(1-20)	1.011	R(6-13)	1.094
R(2-3)	1.512	R(6-14)	1.094
R(2-6)	1.538	R(6-15)	1.095
R(2-10)	1.096	R(7-8)	1.394
R(2-11)	1.095	R(7-16)	1.084
R(3-4)	1.398	R(8-17)	1.088
R(3-18)	1.348	R(8-18)	1.337
R(4-5)	1.399	R(9-21)	1.684
R(4-12)	1.084		

Bond Angles(^{o})

A(9-1-19)	121.9	A(3-4-5)	119.7
A(9-1-20)	119.9	A(3-4-12)	120.4
A(1-9-5)	115.3	A(3-18-8)	118.0
A(1-9-21)	122.4	A(5-4-12)	119.8
A(19-1-20)	117.9	A(4-5-7)	118.0
A(3-2-6)	112.5	A(4-5-9)	120.9

Table 3.5 (continued): Calculated geometry parameters of ETH.

A(3-2-10)	108.3	A(7-5-9)	121.1
A(3-2-11)	109.5	A(5-7-8)	118.3
A(2-3-4)	121.4	A(5-7-16)	121.7
A(2-3-18)	116.5	A(5-9-21)	122.2
A(6-2-10)	109.2	A(13-6-14)	108.3
A(6-2-11)	109.9	A(13-6-15)	108.1
A(2-6-13)	110.6	A(14-6-15)	108.1
A(2-6-14)	110.6	A(8-7-16)	119.9
A(2-6-15)	111.1	A(7-8-17)	119.7
A(10-2-11)	107.2	A(7-8-18)	124.0
A(4-3-18)	122.0	A(17-8-18)	116.4

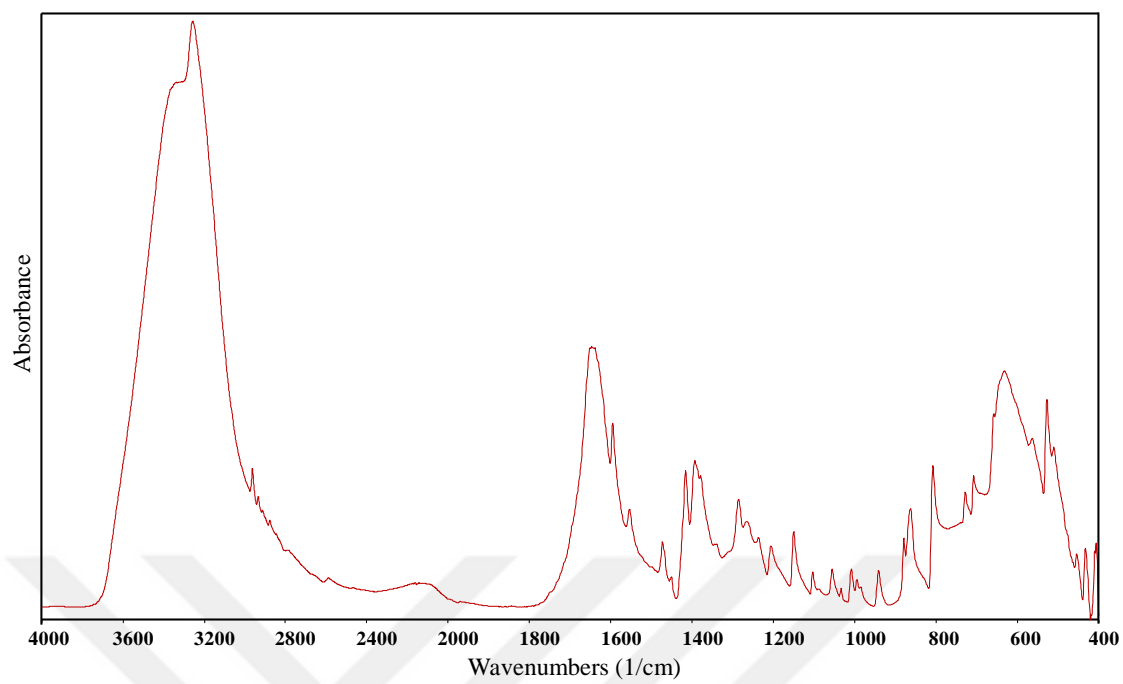A: Bond angle, R: Bond distance.

Figure 3.11: FTIR spectra of ETH-water complex.

Table 3.6: Comparison of the experimental wavenumbers (cm^{-1}) and theoretical harmonic frequencies (cm^{-1}) of ETH calculated by the B3LYP method using 6-31G (d,p) basis set.

Wavenumbers Experimental – IR		Wavenumbers calculated	PED($\geq$10%)
ETH	ETH-water		
		32	(91)τ(CC)
		49	(88)τ(CC)
		121	(35)γ(CC), (27)τ_{ring} , (11)τ(CC), (10)δ(CCC)
		141	(22)τ_{ring} , (20)δ(CC), (10)δ(CCN), (10)δ(CS), (10)γ(CC), (10)δ(CCC), (10)γ(CC)
		169	(23)δ(CC), (20)τ_{ring} , (13)τ(CC), (10)γ(CC), (10)δ(CC), (10)γ(CS)
		227	(70)τ(CC), (10)δ(CC)
		297	(47)τring , (37)δ(CCC)
		309	(38)δ(CS), (15)δring , (14)ν(CC), (10)δ(CC)
		345	(36)δ(CCN), (30)δ(CC), (10)τ(CC)
		403	(39)τ_{ring} , (20)δ(CC), (10)δ(CCN), (10)γ(CS)
		473	(83)NH$_2$ wagging , (14)τ(NC)
		485	(38)τ_{ring} , (18)δ(CCN), (9)ν(CS)
		510	(42)δ_{ring} , (21)δ(CS), (10)τ_{ring}
529	528	544	(18)**δ_{ring}** , (10)ν(CC), (10)ν(CC)ring , (10)δ(CS), (10)τ_{ring} , (10)γ(CS), (10)δ(CC)
565	564	592	(28)**δ_{ring}** , (15)τ(NC), (15)τ_{ring} , (12)γ(CS), (10)δ(CCC)
		637	(62)τ(NC), (15)NH$_2$ wagging , (14)γ(CS)
637	634	700	(51)**δ_{ring}** , (11)ν(CS)

Table 3.6 (continued): Comparison of the experimental wavenumbers (cm^{-1}) and theoretical harmonic frequencies (cm^{-1}) of ETH calculated by the B3LYP method using 6-31G (d,p) basis set.

729	729	720	(32)**γ(CS),** (23)γ(CC), (15)γ(CC)
		770	(71)τ$_{ring}$, (10)γ(CC)
		796	(46)CH$_2$ rocking, (36)δ(CCH$_3$)
808	808	841	(23)**ν(CS),** (17)**δ$_{ring}$** , (16)ν(CC), (10)ν(CC)$_{ring}$, (10)δ(CCH3)
879	879	870	(89)**γ(CH)$_{ring}$** , (10)γ(CC)
		924	(24)NH$_2$ rocking, (20)ν(CS), (12)ν(CC), (11)ν(CC)$_{ring}$, (10)ν(CC), (10)δ$_{ring}$
942	942	932	(91)**γ(CH)$_{ring}$**
		990	(29)ν(CN)$_{ring}$, (27)δ$_{ring}$, (17)ν(CC)$_{ring}$, (14)ν(CC)
		995	(35)ν(CC), (28)δ$_{ring}$, (10)ν(CC)$_{ring}$, (10)δ(CCH3)
995	995	1012	(100)**γ(CH)$_{ring}$**
1009	1009	1072	(31)**δ(CCH$_3$),** (19)CH$_2$ rocking , (16)CH$_2$ twisting , (13)ν(CC)ring
		1087	(48)δ(CCH3), (19)ν(CC), (10)δ(CCC), (10)γ(CC)
1056	1056	1141	(33)**ν(CC)$_{ring}$** , (24)**NH$_2$ rocking**, (23)**δ(CH)$_{ring}$**
1103	1103	1150	(48)**δ(CH)$_{ring}$** , (27)**ν(CC)$_{ring}$**
1150	1150	1238	(28)**δ(CH)$_{ring}$** , (11)ν(CC), (10)**ν(CC)$_{ring}$** , (10)**NH$_2$ rocking**, (10)**CH$_2$ wagging**
		1269	(37)CH$_2$ twisting , (18)δ(CCH$_3$), (10)δ(CH)$_{ring}$, (10)ν(CN)$_{ring}$
		1300	(32)ν(CC)$_{ring}$, (20)ν(CN)$_{ring}$, (11)ν(C=N), (10)CH$_2$ twisting

Table 3.6 (continued): Comparison of the experimental wavenumbers (cm^{-1}) and theoretical harmonic frequencies (cm^{-1}) of ETH calculated by the B3LYP method using 6-31G (d,p) basis set.

1206	1206	1319	(28)**ν(CN)$_{ring}$** , (26)δ(**CH**)$_{ring}$, (23)CH$_2$ wagging , (10)**ν(CC)$_{ring}$**
		1340	(33)δ(CH)$_{ring}$, (21)CH$_2$ wagging , (10)ν(CN)$_{ring}$, (10)CH$_2$ twisting
		1363	(18)CH$_2$ wagging , (10)δ(CH)ring , (10)NH$_2$ rocking, (10)ν(CC), (10)ν(CN)$_{ring}$, (10)ν(CS)
1285	1286	1409	(48)**ν(C=N),** (13)δ(CH)$_{ring}$, (12)ν(CC), (10)ν(CC)$_{ring}$
		1411	(97)δ(CCH$_3$)
		1452	(37)ν(CC)$_{ring}$, (16)δ(CH)$_{ring}$, (10)ν(CC)
1379	1379	1486	(79)**CH$_2$ scissoring**, (18)δ(CCH$_3$)
1393	1393	1500	(98)**δ(CCH$_3$)**
1451	1451	1514	(66)δ(CCH$_3$), (14)CH$_2$ scissoring, (10)δ(CH)$_{ring}$
1472	1473	1518	(43)**δ(CH)$_{ring}$** , (18)**ν(CN)$_{ring}$** , (15)δ(CCH$_3$), (14)**ν(CC)$_{ring}$**
1553	1553	1599	(43)**ν(CC)$_{ring}$** , (27)**ν(CN)$_{ring}$** , (10)NH$_2$ scissoring, (10)δ(CH)$_{ring}$, (10)δ$_{ring}$
1595	1595	1643	(59)**ν(CC)$_{ring}$** , (17)δ(CH)$_{ring}$, (10)δ$_{ring}$, (10)ν(CN)$_{ring}$
1652	1652	1647	(79)**NH$_2$ scissoring**, (10)ν(C=N)
		3047	(100)ν(CH$_3$)
2877	2877	3053	(99)**ν(CH$_2$)**
2912	2913	3097	(80)**ν(CH$_2$),** (21)**ν(CH$_3$)**
2935	2935	3121	(89)**ν(CH$_3$)**, (11)**ν(CH$_2$)**
		3173	(100)ν(CH)

Table 3.6 (continued): Comparison of the experimental wavenumbers (cm⁻¹) and theoretical harmonic frequencies (cm⁻¹) of ETH calculated by the B3LYP method using 6-31G (d,p) basis set.

		3217	(100)ν(CH)
3064	3065	3221	(100)**ν(CH)**
3256	3257	3572	(100)**ν(NH₂)**
	3365	3702	(100)**ν(NH₂)**

ν, stretching; δ, in-plane bending; γ, out-of-plane bending; τ, torsional.

4. DISCUSSION

In this study; the lowest energetic geometry and vibrational frequencies of ETH molecule and H_2O complexes are calculated using Gaussian 09 software with DFT / B3LYP with 6-31G (d, p) basis set.

Wave numbers and experimental wave number values calculated for the most stable structure of ETH are given in Table 3.6. Optimized geometry parameters of ETH molecule and ETH-H_2O complexes are given in Table 3.1-3.5. Free energy of ETH molecule is found to be -8.607712487 a.u. Energy values of possible water complexes are found as -895.027888958 a.u., -895.028096376 a.u., -971.467567932 a.u and -895.034306954 a.u. respectively. Energy values of water complexes of ETH molecule are found lower than free ETH molecule and this fact shows us that water complexes are more stable than the free molecule.

Hydrogen bonds of possible four water complexes of free ETH molecule with water molecule are determined. Lengths of these hydrogen bonds are shown in Figure 3.1, Figure 3.3, Figure 3.1.5, and Figure 3.7. Lengths of hydrogen bonds in ETH-H_2O complex are found to be 1,951 Ǻ, 1,927 Ǻ, 1,944 Ǻ, 1,894 Ǻ and 1,860 Ǻ. respectively. These results show us that the hydrogen bonds formed are strong.

optimized geometry parameters of free ethionamide (ETH) molecule and its possible ethionamide-water complexes were determined by using DFT/ B3LYP with 6-31G(d,p) basis set. After geometry optimization calculation, the harmonic vibrational wavenumbers and IR intensities of the most stable ETH molecule and its water complexes were calculated. The assignment of the vibrational modes was performed based on the potential energy distribution (PED). FTIR (Fourier Transform Infrared) spectra of the ETH and ETH-water complex were recorded with an ATR (Attenuated Total Reflectance) unit in the regions 4000-400 cm^{-1} in the solid phase. By comparing the experimental and theoretical obtained spectra, the variations in wavenumbers and intensity were examined.

5. CONCLUSION AND RECOMMENDATIONS

In this thesis, it is observed that the most significant change in IR spectra of ETH-H_2O complexes due to hydrogen bond effect occurred in vibrational modes of the amide group and in vibrational modes of the ring.

Spectroscopy examines the interaction of light with the matter. Molecules make vibration, rotation, and reciprocating motion. Examination of intramolecular vibrational and rotational movements gives important information about the structure of molecules. The structure and the structural changes in any compound can be examined by the Infrared Spectroscopy method. The region 1200-600 cm^{-1} in Infrared Spectrum is called the fingerprint region and the region between 3600-1200 cm^{-1} is called the functional group which gives structural changes.

In theoretical part of this thesis, stable geometry and vibrational frequencies of Ethionamide (ETH) molecule and its H_2O complexes were calculated by Gaussian 09 program with Density Functional Theory (DFT) method with 6-31G (d, p) basis set. In the experimental part of this study, FT-Mid IR spectra of the ETH ad ETH-water complex were recorded in the regions 4000-400 cm^{-1} in the solid phase. The comparison between calculated and experimental vibrational spectra and assignments of fundamental vibrational modes were characterized by Potential Energy Distribution (PED).

REFERENCES

Baiardi, A., Bloino, J., & Barone, V., 2016, General formulation of vibronic spectroscopy in internal coordinates, *The Journal of Chemical Physics*, 144(8), 084114.

Banerjee, A., Dubnau, E., Quemard, A., Balasubramanian, V., Um, K. S., Wilson, T., Jacobs, W. R., 1994, inhA, a gene encoding a target for isoniazid and ethionamide in Mycobacterium tuberculosis, *Science*, 263(5144), 227-230.

Chan, K. A., & Kazarian, S. G., 2016, Attenuated total reflection Fourier-transform infrared (ATR-FTIR) imaging of tissues and live cells. *Chemical Society Reviews*, 45(7), 1850-1864.

Colthup, N., 2016, *Introduction to infrared and Raman spectroscopy*, Elsevier.

Dyall, K. G., 2012, *One-Particle Basis Sets for Relativistic Calculations*, Handbook of Relativistic Quantum Chemistry, 1-24.

Dye, C., Scheele, S., Dolin, P., Pathania, V., Raviglione, M. C., 1999, Global burden of tuberculosis: estimated incidence, prevalence, and mortality by country, *Jama*, 282(7), 677-686.

Faix, O., 1992, *Fourier transform infrared spectroscopy Methods in lignin chemistry*, Springer, 83-109.

Frisch, M. J., Trucks, G. W., Schlegel, H. B., Scuseria, G. E., Robb, M. A., Cheeseman, J. R., Scalmani, G., Barone, V., Mennucci, B., Petersson, G. A., Nakatsuji, H., Caricato, M., Li, X., Hratchian, H. P., Izmaylov, A. F., Bloino, J., Zheng, G., Sonnenberg, J. L., Hada, M., Ehara, M., Toyota, K., Fukuda, R., Hasegawa, J., Ishida, M., Nakajima, T., Honda, Y., Kitao, O., Nakai, H., Vreven, T., Montgomery, J. A., Jr., Peralta, J. E., Ogliaro, F., Bearpark, M., Heyd, J. J., Brothers, E., Kudin, K. N., Staroverov, V. N., Kobayashi, R., Normand, J., Raghavachari, K., Rendell, A., Burant, J. C., Iyengar, S. S., Tomasi, J., Cossi, M., Rega, N., Millam, J. M., Klene, M., Knox, J. E., Cross, J. B., Bakken, V., Adamo, C., Jaramillo, J., Gomperts, R., Stratmann, R. E., Yazyev, O., Austin, A. J., Cammi, R., Pomelli, C., Ochterski, J. W., Martin, R. L., Morokuma, K., Zakrzewski, V. G., Voth, G. A., Salvador, P., Dannenberg, J. J., Dapprich, S., Daniels, A. D., Farkas, Ö., Foresman, J. B., Ortiz, J. V., Cioslowski, J., Fox, D. J., Gaussian 09, Revision A.02, Gaussian Inc., Wallingford CT, 2009.

Hamilton, C. D., 1999, Recent developments in epidemiology, treatment, and diagnosis of tuberculosis, *Current infectious disease reports*, 1(1), 80-88.

Hehre, W. J., 2003, *A guide to molecular mechanics and quantum chemical calculations*, Wavefunction Irvine, CA, 2.

Hershfield, E. S., 1991, Tuberculosis–Still a major health problem, *Canadian Journal of Infectious Diseases and Medical Microbiology*, 2(4), 131-132.

Jaggi, N., Vij, D., 2006, *Fourier transform infrared spectroscopy Handbook of Applied Solid State Spectroscopy*, Springer, 411-450.

Jensen, F., 2017, *Introduction to computational chemistry*, John wiley & Sons.

Jmol: An open-source Java viewer for chemical structures in 3D, version 13.0, 2018, http://www.jmol.org/.

Jones, R. O.,2015, Density functional theory: Its origins, rise to prominence, and future, *Reviews of modern physics*, 87(3), 897.

Kaminski, G. A., Friesner, R. A., Tirado-Rives, J., Jorgensen, W. L., 2001, Evaluation and reparametrization of the OPLS-AA force field for proteins via comparison with accurate quantum chemical calculations on peptides, *The Journal of Physical Chemistry B*, 105(28), 6474-6487.

Kato, T., Ide, Y., Yamanouchi, K., 2015, Molecular wave function and effective adiabatic potentials calculated by extended multi-configuration time-dependent Hartree-Fock method, *AIP Conference Proceedings*.

Kazarian, S. G., Chan, K. A., 2010, Micro-and macro-attenuated total reflection Fourier transform infrared spectroscopic imaging, *Applied spectroscopy*, 64(5), 135A-152A.

Khasnobis, S., Escuyer, V. E., Chatterjee, D. (2002). Emerging therapeutic targets in tuberculosis: post-genomic era, *Expert opinion on therapeutic targets*, 6(1), 21-40.

King, A. W., Baskerville, A. L., Cox, H. (2018). Hartree–Fock implementation using a Laguerre-based wave function for the ground state and correlation energies of two-electron atoms, *Phil. Trans. R. Soc. A*, 376(2115), 20170153.

Koch, W., Holthausen, M. C., 2015, *A chemist's guide to density functional theory*, John Wiley & Sons.

Larkin, P., 2017, *Infrared and Raman spectroscopy: principles and spectral interpretation*, Elsevier.

Long, D. A., 1977, *Raman spectroscopy*, McGraw-Hill, New York.

Martin, J.M.L., Alsenoy, C.V., Gar2PED, University of Antwerp, Antiwerp, 1995.

Medvedev, M. G., Bushmarinov, I. S., Sun, J., Perdew, J. P., Lyssenko, K. A., 2017, Density functional theory is straying from the path toward the exact functional, *Science*, 355(6320), 49-52.

Min, S. K., Abedi, A., Kim, K. S., & Gross, E., 2014, Is the molecular Berry phase an artifact of the Born-Oppenheimer approximation?, *Physical review letters*, 113(26), 263004.

Muthu, S., Ramachandran, G., 2012, Vibrational spectroscopic investigation on the structure of 2-ethylpyridine-4-carbothioamide, *Spectrochimica Acta Part A: Molecular and Biomolecular Spectroscopy*, 93, 214-222.

Perdew, J. P., Yang, W., Burke, K., Yang, Z., Gross, E. K., Scheffler, M., Ruzsinszky, A., 2017, Understanding band gaps of solids in generalized Kohn–Sham theory, *Proceedings of the National Academy of Sciences*, 114(11), 2801-2806.

Qiu, Y., Henderson, T. M., Scuseria, G. E., 2017, Projected Hartree-Fock theory as a polynomial of particle-hole excitations and its combination with variational coupled cluster theory, *The Journal of Chemical Physics*, 146(18), 184105.

Quemard, A., LaCave, C., Laneelle, G., 1991, Isoniazid inhibition of mycolic acid synthesis by cell extracts of sensitive and resistant strains of Mycobacterium aurum, *Antimicrobial agents and chemotherapy*, 35(6), 1035-1039.

Roos, B. O., Lindh, R., Malmqvist, P. Å., Veryazov, V., Widmark, P. O., 2016, *Basis Sets*, Multiconfigurational Quantum Chemistry, 69-84.

Sathyanarayana, D. N., 2015, *Vibrational spectroscopy: theory and applications*, New Age International.

Schäfer, A., Huber, C., Ahlrichs, R., 1994, Fully optimized contracted Gaussian basis sets of triple zeta valence quality for atoms Li to Kr, *The Journal of Chemical Physics*,100(8), 5829-5835.

Scherrer, A., Agostini, F., Sebastiani, D., Gross, E., Vuilleumier, R., 2017, On the mass of atoms in molecules: Beyond the Born-Oppenheimer approximation, *Physical Review*, 7(3), 031035.

Schroeder, E., de Souza, O. N., Santos, D., Blanchard, J., Basso, L., 2002, Drugs that inhibit mycolic acid biosynthesis in Mycobacterium tuberculosis, *Current pharmaceutical biotechnology*, 3(3), 197-225.

Sittel, F., Jain, A., & Stock, G., 2014, Principal component analysis of molecular dynamics: On the use of Cartesian vs. internal coordinates, *The Journal of Chemical Physics*, 141(1), 07B605_601.

Slater, J. C., 1951, A simplification of the Hartree-Fock method, *Physical Review*, 81(3), 385.

Smith, B. C., 2011, *Fundamentals of Fourier transform infrared spectroscopy*, CRC press.

Umar, A., Oberacker, V., Simenel, C., 2015, Shape evolution and collective dynamics of quasifission in the time-dependent Hartree-Fock approach, *Physical Review C*, 92(2), 024621.

Wollrab, J. E., 2016, Rotational Spectra and Molecular Structure: Physical Chemistry: A Series of Monographs, *Academic Press*, 13.

Woodward, L. A., 1972, *Introduction to the theory of molecular vibrations and vibrational spectroscopy*, Oxford University Press.

Woolley, R., & Sutcliffe, B., 1977, Molecular structure and the Born-Oppenheimer approximation, *Chemical Physics Letters*, 45(2), 393-398.

Wysokiński, R., Michalska, D., Bieńko, D., Ilakiamani, S., Sundaraganesan, N., Ramalingam, K., 2006, Density functional study on the molecular structure, infrared and Raman spectra, and vibrational assignment for 4-thiocarbamoylpyridine, *Journal of Molecular Structure*, 791(1-3), 70-76.

Zaman, K., 2010, Tuberculosis: a global health problem, *Journal of health, population and nutrition*, 28(2), 111.

Yilmaz, A., & Bolukbasi, O., 2016, Molecular structure and vibrational spectroscopic studies of prothionamide by density functional theory, *Spectrochimica Acta Part A: Molecular and Biomolecular Spectroscopy*, 152, 262-271

Yilmaz, A., Bolukbasi, O., Bakiler, M., 2008, An experimental and theoretical vibrational spectra of isoniazide, *Journal of Molecular Structure*, 872(2-3), 182-189.

Bakiler, M., Bolukbasi, O., Yilmaz, A., 2007, An experimental and theoretical study of vibrational spectra of picolinamide, nicotinamide, and isonicotinamide, *Journal of Molecular Structure*, 826(1), 6-16.

CURRICULUM VITAE

Personal Information	
Name Surname	Umaima Saleh Mahfouth ZERT
Place of Birth	Tripoli
Date of Birth	09.07 2018
Nationality	❏ T.C. ❏ Other:
Phone Number	05347014405
Email	omimazarti@gmail.com
Web Page	

Educational Information	
B. Sc.	
University	Higher Institute for Medical Professions
Faculty	Engineering
Department	Optical Engineering
Graduation Year	07.09.2018

M. Sc.	
University	İstanbul University
Institute	İnstıtute Of Graduate Studies In Science And Engineering
Department	Physics
Programme	Physics